# Evaluation of Historic and Operational Satellite Radar Altimetry Missions for Constructing Consistent Long-term Lake Water Level Records

Song Shu[1*], Hongxing Liu[2*], Richard A. Beck[3], Frédéric Frappart[4], Johanna Korhonen[5],Minxuan Lan[3], Min Xu[6], Bo Yang[7], Yan Huang[8]

[1]Department of Geography and Planning, Appalachian State University, Boone, NC 28608, USA
[2]Department of Geography, the University of Alabama, Tuscaloosa, AL 35487, USA
[3]Department of Geography and Geographic Information Science, University of Cincinnati, Cincinnati, OH 45221, USA
[4]Laboratoire d'Etudes en Géophysique et Océanographie Spatiales (LEGOS), UMR 5566, CNRS/IRD/UPS, OMP, 14 Avenue Édouard Belin, 31400 Toulouse, France
[5]Finnish Environment Institute, SYKE, Freshwater Center, Latokartanonkaari 11, 00790 Helsinki, Finland
[6]College of Marine Science, University of South Florida, St. Petersburg, FL 33701, USA
[7]Department of Sociology, University of Central Florida, Orlando, FL 32816, USA
[8]Key Lab. of Geographical Information Science, Ministry of Education, School of Geographical Science, East China Normal University, Shanghai 200241, China

*Correspondence to*: Song Shu (shus@appstate.edu), Hongxing Liu (Hongxing.Liu@ua.edu)

**Abstract.** Thirteen satellite missions have been launched since 1985, with different types of radar altimeters onboard. This study intends to make a comprehensive evaluation of historic and currently operational satellite radar altimetry missions for lake water level retrieval over the same set of lakes and to develop a strategy for constructing consistent long-term water level records for inland lakes at global scale. The lake water level estimates produced by different retracking algorithms (retrackers) of the satellite missions were compared with the gauge measurements over twelve lakes in four countries. The performance of each retracker was assessed in terms of the data missing rate, the correlation coefficient r, the bias, and the Root Mean Square Error (*RMSE*) between the altimetry-derived lake water level estimates and the concurrent gauge measurements. The results show that the model-free retrackers (e.g. OCOG/Ice-1/Ice) outperform the model-based retrackers for ~~all~~ most of the missions, particularly over small lakes. Among the satellite altimetry missions, Sentinel-3 gave the best results, followed by SARAL. ~~ENVISat~~ENVISAT has slightly better lake water level estimates than Jason-1 and -2, but its data missing rate is higher. For small lakes, ERS-1 and ERS-2 missions provided more accurate lake water level estimates than Topex/Poseidon mission. In contrast, for large lakes Topex/Poseidon is a better option due to its lower data missing rate and shorter repeat cycle. GeoSat and GeoSat Follow-On (GFO) both have extremely high data missing rate of lake water level estimates. Although several contemporary radar altimetry missions provide more accurate lake level estimates than GFO, GeoSat was the sole radar altimetry mission between 1985 and 1990 that provided the lake water level estimates. With a full consideration of the performance and the operational duration, the best strategy for constructing long-term lake water

35 level records should be a two-step bias correction and normalization procedure. In the first step, use Jason-2 as the initial reference to estimate the systematic biases with Topex/Poseidon, Jason-1 and Jason-3 and then normalize them to form a consistent Topex/Poseidon-Jason series. Then, use Topex/Poseidon-Jason series as the reference to estimate and remove systematic biases with other radar altimetry missions to construct consistent long-term lake water level series for ungauged lakes.

## 1 Introduction

About three percent of Earth's land surface is covered by lakes (Pekel et al., 2016). These lakes are the habitats for a great number of aquatic and terrestrial species (Schindler and Scheuerell, 2002). They are also the major freshwater sources for various human activities (Postel et al., 1996). The long-term variations of lake water levels were identified as sentinel for climate change (Adrian et al., 2009;Williamson et al., 2009). The lake water level change can also have significant
45 influences on the local ecosystem and environment, e.g. the breeding success of fishes (Probst et al., 2009), the drainage of thaw lakes (Pohl et al., 2009;Marsh et al., 2009;Jones and Arp, 2015) and landslide at lake coastal areas (Tyszkowski et al., 2015). Monitoring lake water levels is important for a better understanding of their impact on the environment and for the wise management of freshwater resources.

At present, only a very small portion of lakes are monitored by gauge stations. The number of gauged lakes has decreased in
50 recent years owing to the high cost of installation and maintenance of gauge stations (Hannah et al., 2011). The overwhelming majority of the lakes on Earth remain ungauged, particularly those located in remote areas with harsh environments, e.g. the Arctic and the sub-Arctic regions. Many previous studies show that the lakes in these remote areas have been experiencing dramatic changes with regard to the lake water balance (Turner et al., 2014), the timing and magnitude of spring/early-summer flooding (Rokaya et al., 2018), and the lake ice cover phenology (Surdu et al., 2014), due
55 to the rapid climate warming (Karl et al., 2015). There is an urgent need to develop an alternative approach for effective monitoring of lake water levels at the global scale.

Satellite radar altimeters make surface elevation measurements by tracking the satellite orbit position and the range between the satellite and the Earth's surface at nadir direction. They have been used widely to monitor lake water levels since the 1980s. Thirteen satellite missions have been launched with different radar altimeters onboard in the past three decades.
60 Those include the Geodetic/Geophysical Satellite (GeoSat, 1985 – 1989) (McConathy and Kilgus, 1987) and GeoSat Follow-on (GFO, 1998 – 2008) (Barry et al., 1995) developed by U.S. Navy, ERS-1 (1991 – 2000) (Cheney et al., 1991), ERS-2 (1995 – 2011) (Zandbergen et al., 1997), ~~ENVISat~~ENVISAT (2002 – 2012) (Zelli, 1999), Cryosat-2 (2010 – present) (Wingham et al., 2006) and Sentinel-3 (2016 – present) (Donlon et al., 2012) developed by ESA (European Space Agency), the Satellite with ARgos and ALtika (SARAL, 2013 – present) (Verron et al., 2015) developed jointly by CNES (Centre
65 National d'Etudes Spatiales, the French Space Agency) and ISRO (Indian Space Research Organization), the Topex/Poseidon (T/P, 1992 – 2005) (Lee-Lueng, 1994), Jason-1 (2001 – 2013) (Menard et al., 2003), Jason-2 (2008 –

present) (Lambin et al., 2010) and Jason-3 (2016 – present) developed jointly by NOAA (National Oceanic and Atmospheric Administration), NASA (National Aeronautics and Space Administration), CNES and EUMETSAT (European Organization for the Exploitation of Meteorological Satellites), and the HY-2A (2011 – present) developed by CNSA (China National

70    Space Administration). Most of the radar altimeters operate in a conventional low-resolution mode (LRM), whereas Sentinel-3 and Cryosat-2 operate in Synthetic Aperture Radar (SAR) mode. Cryosat-2 is also able to operate in the interferometric SAR (SARin) mode.

Based on the elevation measurements collected by different satellite radar altimeters, five online databases have also been developed to offer the time series of altimetry-derived water level estimates for major inland lakes around the world. These

75    include the Hydroweb database (http://www.legos.obs-mip.fr/soa/hydrologie/hydroweb/) developed by the Laboratoire d'Etudes en Géophysique et Océanographie Spatiales (LEGOS) (Crétaux et al., 2011), the River and Lake database (http://www.cse.dmu.ac.uk/EAPRS/products_riverlake.html) built by the ESA and De Montfort University (ESA-DMU) (Berry     et     al.,     2005),     the     Global     Reservoir     and     Lake     Monitor     (GRLM, https://ipad.fas.usda.gov/cropexplorer/global_reservoir/) developed by the Foreign Agricultural Service of the United States

80    Department of Agriculture (USDA) (Birkett et al., 2011), the Hydrosat developed by the Institute of Geodesy from the University of Stuttgart (http://hydrosat.gis.uni-stuttgart.de), and the Database for Hydrological Time Series over Inland Waters (DAHITI, https://dahiti.dgfi.tum.de/en/) launched by the Deutsches Geodätisches Forschungsinstitut der Technischen Universität München (DGFI-TUM) in 2013 (Schwatke et al., 2015b). The time series of water level estimates in these databases are produced by merging the elevation measurements from multiple satellite radar altimeters with different

85    processing strategies (Birkett and Beckley, 2010;Ričko et al., 2012;Schwatke et al., 2015b).

For each satellite radar altimeter, one or more dedicated algorithms have been designed to retrieve the surface elevations. Each algorithm is often designed to handle one type of Earth's surface. These radar altimetry algorithms are also known as retracking algorithms or simply *retrackers*. For example, there are four different retrackers designed for ~~ENVISat~~ENVISAT altimeter, including the *Ocean retracker* for ocean open water surface, the *Ice1 retracker* for general continental ice sheet

90    surface, the *Ice2 retracker* for continental internal flat ice surface, and the *Sea-Ice retracker* for ocean ice surface (Frappart et al., 2006).

Many previous studies have evaluated different satellite radar altimeters in the retrieval of water levels over inland lakes with different sizes and environmental surroundings. Morris (1994) examined the performance of GeoSat over the Great Lakes (Erie, Huron, Michigan, Ontario and Superior), and the root mean square error (*RMSE*) between the altimetry-derived water

95    level estimates and the gauge measurements ranged from 9.4 to 13.8 cm. Birkett (1995) assessed Topex/Poseidon over Lake Ontario, Michigan and Superior, and its *RMSE* ranged from 4.69 to 6.2 cm. Also, Birkett *et al.* (2010) evaluated Jason-2 water level estimates against gauge measurements over five lakes. They found that its *RMSE* was 2.95 cm for Lake Ontario (with an area of ~20,000 km$^2$) and 33.2 cm for Lake Yellowstone (with an area of ~350 km$^2$). Frappart *et al.* (2006) investigated the performance of the four retrackers of ~~ENVISat~~ENVISAT over three small lakes (with area from 100 to 300

100    km$^2$) near Curuai in Amazon basin. They observed that the *Ice1 retracker* was the best for retrieving lake water levels with

~~ENVISat~~ENVISAT altimetry observations. Jarihani *et al.* (2013) compared five different satellite radar altimetry missions (~~ENVISat~~ENVISAT, GFO, T/P, Jason-1 and Jason-2) and assessed the performance of different retrackers adopted by these missions over Lake Eildon (138 km²) and Lake Argyle (1000 km²) in Australia. They found out that among the five missions Jason-2 gave the best results with a *RMSE* of 28 cm for Ice1 retracker and 32 cm for MLE3 retracker, while T/P yielded the largest *RMSE* of 150 cm for its sole Ocean retracker. Schwatke *et al.* (2015a) evaluated the performance of ~~ENVISat~~ENVISAT and SARAL over the Great Lakes and found that both missions can achieve very low *RMSE,* ranging from 2 – 6 cm for these large lakes. Villadsen *et al.* (2016) reprocessed Cryosat-2 data with several ~~self-developed~~non-official retrackers and assessed their performance over Lake Vanern (5550 km²) and Lake Okeechobee (1436 km²). They demonstrated that the Multiple Waveform Persistent Peak (MWaPP) retracker produced the lowest *RMSE* of 9.1 cm over Lake Vanern and 13.4 cm over Lake Okeechobee. Cretaux *et al.* (2018) evaluated Sentinel-3 and Jason-3 over Lake Issykkul ( 6236 km²), and found that both missions achieved a very low *RMSE* of 3 cm with the Ocean retracker. Shu *et al.* (2020) assessed the performance of the Sentinel-3 SAR retrackers over fifteen lakes, and they reported that the SAR Altimetry Mode Studies and Applications ~~3~~2 (SAMOSA-~~3~~2) retracker has the lowest mean *RMSE* of 8.08 cm. Jiang *et al.* (2020) also evaluated four retrackers (including official and non-official) for Sentinel-3 and demonstrated that the MWaPP+ retracker can significantly improve the accuracy of water level estimates over large rivers.

Apparently, each of those previous evaluations only focused on a few of radar altimetry missions. Those individual evaluations are not strictly comparable, since each study was conducted over a different set of lakes. The differences in lake's size, geographic location, surrounding topography and land cover types could significantly influence the accuracy of lake water levels retrieved by satellite radar altimeters (Maillard et al., 2015).

Despite the previous research efforts, many questions remain as to the construction of a long-term time series of water level for ungauged inland lakes, particularly for those locate in remote areas (e.g. the Arctic coastal plains). As described above, each radar altimetry mission spans different time periods and has different levels of measurement accuracy, and there exist systematical differences (biases) between different mission measurements. The question is: to construct a long-term consistent time series of lake water level estimates, which radar altimetry mission can be used as a high-confidence initial reference to remove the biases between missions and to tie different missions together? For a certain time period, one lake may be visited by multiple radar missions. In this case, which satellite radar altimetry mission may provide more reliable lake water level estimates? Most of radar altimetry missions have several retrackers that can be used to estimate lake water level. For a given radar altimetry mission, which retracker is most reliable and accurate for lake water level retrieval? The pursuit of answers to these questions entails a comprehensive and consistent evaluation of all radar altimetry missions over the same set of lakes.

In this study, we will examine the performance of all historical and currently operational satellite radar altimetry missions, except for HY-2A and Cryosat-2 missions. HY-2A was excluded from this study because of the difficulty in obtaining its data product (The data is not available online for public access). The exclusion of Cryosat-2 was due to its long repeat cycle orbit that does not allow the production of frequent co-located observations for evaluation. Water level estimates retrieved by

different retrackers of the eleven radar altimetry missions will be assessed by using the corresponding gauge measurements on twelve lakes of various sizes distributed in four countries. After this introductory section, we will briefly describe these lakes and the gauge measurements in Section 2. In Section 3, we will introduce the data sets collected by the eleven satellite radar altimetry missions and the different retrackers adopted by each mission. Then, we present the methods for processing the satellite radar altimetry data to determine lake water levels in Section 4. Next, we evaluate each altimetry mission and its retrackers in comparison with the *gauge* measurements in Section 5 and discuss the performance of each mission and relevant issues in integrating different radar altimetry missions to construct consistent long-term time series in Section 6. The research findings are summarized in Section 7.

## 2 Case study lakes and gauge data

### 2.1 Case study lakes

Our case study sites include twelve lakes/reservoirs in four countries (as shown in Fig. 1). ~~These lakes were selected based on the considerations that they were all overpassed by the eleven satellite radar altimetry missions and they are representative for different sizes, environmental surroundings, and winter ice conditions.~~ The geographic location, the winter ice condition and the gauge station for these lakes are summarized in Table 1. The largest one is Lake Superior in North America (over 80,000 km$^2$), while the smallest one is Reservoir Lokka in Finland (about 500 km$^2$). The three lakes in Finland (Inarijarvi, Lokka, and Oulujarvi) and Lake Cedar in Canada all have numerous islands scattered within the lake, fragmenting the water surfaces of these lakes. Therefore, the surface condition of these lakes is very similar to small lakes, over which the satellite radar altimetry signal is contaminated easily by the surrounding land surfaces. These lakes are treated as small lakes to evaluate the performance of each satellite altimetry mission in contrast to the large lakes (e.g. the Great Lakes, Great Slave Lake, Lake Vanern). The boundary polygons of these twelve lakes were obtained from the Global Lakes and Wetland Databases (GLWD) (Lehner and Döll, 2004). The lake polygons were then used to extract measurements from each mission in the subsequent analysis.

A majority of the lakes on Earth are located between 45°N and 75°N (Verpoorter et al., 2014). ~~These case study lakes~~ Those lakes have varying ice cover conditions in winter seasons, due to the differences in their latitudes and local climates. Among the~~se~~ selected case study lakes, Lake Inarijarvi in Finland is the northernmost with a latitude of 69.02° and Lake Erie is the southernmost with a latitude of 42.16°. The three lakes in Finland and the three lakes in Canada are fully ice-covered in winter seasons. The ice cover usually lasts more than 7 months for Lake Inarijarvi (Korhonen, 2006) and more than 5 months for Great Slave Lake (Howell et al., 2009). The duration of ice cover decreases for the lakes at more southern locations. In comparison with Canadian lakes, the ice cover on Finnish lakes is often much thinner (Shu et al., 2020) due to the heating effect of the North Atlantic Current (Rahmstorf, 2006;Korhonen, 2019).

Lake Vanern in Sweden and the Great Lakes of North America could be fully covered, partly covered, or totally free from ice in winter seasons depending on the winter air temperature. Lake Vanern often remains completely ice-free in winter.

From 1979 to 2002, it was only covered by ice in nine winters (Weyhenmeyer et al., 2008). In a cold winter, Lake Superior and Lake Erie are often fully covered by ice, and the other three (Huron, Ontario, and Michigan) of Great Lakes are partly covered (Assel and Wang, 2017). While in warmer winters, all of them are partly covered.

## 2.2 Gauge data

*In-situ* water level measurements for the twelve lakes were collected respectively at the gauge stations listed in Table 1, which are obtained from four online databases. Those include the Finnish Environment Information Management System – Hertta operated by Finnish Environment Institute (SYKE) (http://www.syke.fi/fi-FI/Avoin_tieto/Ymparistotietojarjestelmat), the SMHI (Swedish Meteorological and Hydrological Institute) website (http://vattenwebb.smhi.se/station/), the Canada Real-time Hydrometric Data Website (https://wateroffice.ec.gc.ca/ mainmenu/real_time_data_index_e.html), and the Center for Operational Oceanographic Products and Services (https://tidesandcurrents.noaa.gov/) operated by NOAA. These gauge stations measure the water-equivalent lake levels when the lake is ice-covered (Shu et al., 2020). Note that the gauge data are referenced to different datums. In this study, only the gauge data on the Great Lakes are converted to EGM2008 using the tool VDatum (https://vdatum.noaa.gov/).

## 3 Satellite radar altimetry data products

In this study, we evaluate the performance of radar altimeters onboard eleven satellite missions. Those include all historical and currently operational satellite radar altimetry missions except for HY-2A and Cryosat-2. No data are available from HY-2A mission launched by China. Cryosat-2 operates on a long-term repeat orbit (369 days) in order to obtain spatially dense coverage in polar regions, and it is difficult to form frequent time series of co-located water level observations for inland lakes. Most of the altimetry data products of the eleven satellite radar altimetry missions have gone through several rounds of updating and refinements. We used the most up-to-date version of data product of each mission for the evaluation. The geographical coverage, operational time period, repeat cycle, ~~footprint size~~sampling rate and retrackers of these radar altimetry missions are summarized in Table 2. The temporal coverage and the overlapping time periods of the eleven missions are illustrated in Fig. 2.

Satellite radar altimeters measure elevation through transmitting radar signal pulses to the nadir surface and timing the echoes. The transmitted and echoed radar pulse is sampled as pulse strength over the elapsed time, which is known as radar altimetry "waveform". Most of the eleven missions (except for GeoSat, Topex/Poseiden and GFO) adopted two or more retracking algorithms (retrackers) to process the echoed waveforms in order to produce accurate elevation measurements for different types of Earth's surfaces. These retrackers can be divided into two general categories: the empirical/model-free retrackers and the physical/model-based retrackers. The model-based retrackers fit a physically based model to the echoed waveform to produce elevation measurements. For example, the ~~ENVISat~~ENVISAT Ocean retracker is based on the Brown model (1977) and the Sentinel-3 Ice-Sheet retracker~~s~~ is based on a 5-part piecewise analytical function (MSSL/UCL/CLS,

2019). The model-free retrackers have no assumption on the model of the echoed waveform, and the examples include Offset Center of Gravity (OCOG, also known as Ice1 or Ice) developed by Wingham (1986) and the Sea-Ice retracker developed by Laxon (1994). There are also many efficient non-official retrackers (model-based or model-free) developed in previous studies for different surface conditions (Jiang et al., 2020). In this study, we only focus on the official retrackers that were adopted by each mission to generate the official data products.

Ten of the eleven missions (except for Sentinel-3) utilize the conventional pulse-limited altimeter to measure surface elevation. The diameter of the radar pulse footprint on Earth's surface varies from 1.6 km to 13.4 km, according to the satellite orbit, the echoing surface roughness and the duration of radar pulse (Chelton et al., 1989). Among the ten conventional pulse-limited altimetry missions, SARAL utilizes a Ka-band (35.75 GHz) as the primary band with a bandwidth of 480 MHz to measure Earth's surface elevation, while the others use Ku-band (e.g. 13.6 GHz) as the primary band with a bandwidth of 320 MHz. Due to the adoption of the Ka band and the higher bandwidth, the footprint generated by SARAL is about 0.8 times smaller than the other Ku-band altimeters for a given pulse length and orbit altitude (Raney and Phalippou, 2011). Sentinel-3 uses a synthetic aperture radar (SAR) altimeter to measure Earth's surface elevation. This SAR altimetry technology decreases the along-track footprint size from several kilometers to about 300 m, which improves the retrieval of elevation information over more variable surfaces, e.g. coastal areas (Donlon et al., 2012).

*GeoSat* was launched on March 12, 1985 by U.S. Navy, and its operations consisted of two distinct mission phases: the Geodetic Mission (GM) and the Exact Repeat Mission (ERM) (McConathy and Kilgus, 1987). The GM phase lasted about 18 months from March 31, 1985 to September 30, 1986 and the ERM phase lasted about 3.5 years from November 8, 1986 to January 1990. In the GM phase, the satellite operated on a geodetic drifting orbit, while in the ERM phase, it operated on an exact-repeat orbit with a repeat cycle of 17 days. In both phases, the satellite collected elevation measurements of Earth's surface between 72°N and 72°S latitudes. GeoSat used a single ocean retracker based on the Brown (1977) model to produce elevation measurements for all different types of Earth's surface (Lillibridge et al., 2006). The georeferenced measurements were originally provided at a 1 Hz rate by the National Centers for Environmental Information (NCEI) at NOAA (https://accession.nodc.noaa.gov/0053056). For this study, we obtained GeoSat data from the Radar Altimeter Database System (RADS) (Scharroo et al., 2013). RADS provides the most up-to-date harmonized geophysical and systematic corrections for all the satellite radar altimeters. The limitation of RADS is that all the data are provided only at 1 Hz rate. Since the original georeferenced data was also at the 1 Hz rate, the RADS GeoSat data product, instead of the NOAA/NCEI product, was therefore chosen for the evaluation. At the 1 Hz data rate, the sampling interval along the satellite track is $6 - 7$ km depending on the latitude. *GeoSat Follow-On* (GFO) was launched on February 10, 1998 and ended on October 22, 2008. Since it was a follow-on mission of GeoSat, it retained the GeoSat ERM orbit with a repeat cycle of 17 days and covered Earth's surface between 72°N and 72°S latitudes along the satellite ground tracks (Office and Altimetry, 2002). The elevation measurements were produced by the same retracking algorithm used for GeoSat. The georeferenced data was provided at a 10 Hz rate and distributed by U.S. Navy and NOAA at https://accession.nodc.noaa.gov/0085960. With the 10 Hz sampling rate, the distance between two adjacent measurements is about 700 m.

*ERS-1* and *ERS-2* were launched by ESA on July 17, 1991 and April 21, 1995, and retired on March 10, 2000 and September 5, 2011, respectively (Duchossois and Martin, 1995). ERS-2 was the tandem mission of ERS-1 and carried basically the same set of instruments onboard ERS-1. ERS-1 had eight mission phases (Phase A, B, R, C, D, E, F, and G) with different
235  repeat cycles during its lifetime (http://www.deos.tudelft.nl/ers/phases), including the 3-day cycle for the commissioning and the ice phases (Phase A, B, and D), the 35-day cycle for the nominal observation phase (Phase R, C and G), and the 168-day cycle for the geodetic drifting phases (Phase E and F). ERS-2 had two phases: the 35-day nominal observation phase (from April 29, 1995 to February 21, 2011) and the 3-day phase (from March 10, 2011 to July 6, 2011). Elevation measurements collected by both missions cover Earth's surface between 81.5°N and 81.5°S latitude (Brockley, 2014). After the retirement
240  of ERS-2, the data collected by the two missions between August 1991 and July 2003 were reprocessed to generate an improved homogeneous long-term dataset, which is called the REAPER (the Reprocessing of Altimeter Products for ERS) products (Brockley et al., 2017). In the reprocessing, the four retrackers used for ENVISATENVISAT (*Ocean, Ice1, Ice2* and *Sea-Ice*) were adopted to refine elevation measurements. *Ice1* and *Sea-Ice* are model-free retrackers developed by Wingham (1986) and Laxon *et al.* (1994). The other two are model-based retrackers. Later, the ERS-2 data were further reprocessed by
245  the Centre de Topographie des Océans et de l'Hydrosphère (CTOH) at the Laboratoire d'Etudes en Géophysique etOcéanographie Spatiales (LEGOS) (Frappart et al., 2016). The CTOH ERS-2 product contains elevation measurements generated by two retrackers: *Ice1* and *Ice2*. In this study, we chose the ERS-1 REAPER data product from ESA (https://earth.esa.int/) and the further improved ERS-2 data product from CTOH (http://ctoh.legos.obs-mip.fr/) for the evaluation. Both products provide georeferenced elevation measurements at a 20 Hz rate. At this data rate, the distance
250  between two adjacent measurements along the satellite track is about 350 m.

*ENVISATENVISAT* was launched on February 28, 2002, as the successor to ERS-1 and ERS-2. In the nominal observation phase, ENVISATENVISAT operated on the same orbit as ERS-1 and ERS-2 with a 35-day repeat cycle from 2002 to 2010. In October 2010, it was maneuvered to a new orbit with a repeat cycle of 30 days to extend its mission lifetime, until April 08, 2012. This new phase is referred to as "Extension Phase". In both phases, the elevation measurements were provided at an
255  18 Hz rate with a sampling interval of about 370 m along the satellite ground track. ENVISATENVISAT mission used four retrackers (Ocean, Ice1, Ice2, and Sea-Ice) to generate elevation measurements for different types of Earth's surface. In 2018, the ENVISATENVISAT altimetry data were reprocessed and released by ESA as the ENVISATENVISAT V3 product. We obtained this most recent Version 3 product from ESA (https://earth.esa.int/) for the evaluation.

*SARAL* is a joint altimetry mission of CNES (Space Agency of France) and ISRO (Indian Space Research Organization). It
260  was launched on February 25, 2013 by ISRO and is the first satellite mission with a Ka-band (35.75 GHz) radar altimeter onboard (Frappart et al., 2015;Bonnefond et al., 2018). During its exact repetitive phase from the launch to July 4, 2016, SARAL flew on ENVISATENVISAT nominal orbit with a 35-day exact repeat cycle. Due to technical issues with the reaction wheels, the repetitive orbit was no longer maintained since July 4, 2016 and the orbit of the satellite decayed naturally, leading to irregular drifting ground tracks on Earth's surface. This new phase is known as "SARAL Drifting
265  Phase" (Dibarboure et al., 2018). The four ENVISATENVISAT retrackers (Ice1, Ice2, Sea-Ice and Ocean) were adopted by

SARAL in the creation of different data products for different types of Earth's surfaces. The data are provided at a rate of 40 Hz by AVISO+ (Archiving, Validation and Interpretation of Satellite Oceanographic data, ftp://avisoftp.cnes.fr/AVISO/pub/) at the CNES (https://aviso-data-center.cnes.fr/). The distance between two adjacent measurements along the satellite track is about 180 m. In this study, we only evaluated the SARAL data collected in the exactly repetitive phase.

*Topex/Poseidon (T/P)*, *Jason-1*, *Jason-2* and *Jason-3* are four continuous missions that provide long-term consistent altimetry observations of Earth's surface along the same fixed ground tracks. The operation of each satellite is usually composed of two phases: the phase with nominal orbit and the phase with interleaved orbit (Fu et al., 1994). Both orbits have an exact repeat cycle of 10 days and cover Earth's surface between 66°N – 66°S latitudes. Each satellite in this series firstly flies on the nominal orbit after launch, and was usually maneuvered to a new orbit, a number of months after the launch of its successor satellite. The ground tracks generated by this new orbit phase are on the midway between its nominal ground tracks, hence the new orbit is referred to as interleaved orbit. The period between the launch of the successor satellite and the maneuver of the predecessor satellite is often called tandem phase. During this phase, the two satellites fly on the same orbit separated by 60 – 70 seconds (see Jason-3 Products Handbook). Topex/Poseiden was launched on August 10, 1992 and then maneuvered to the interleaved orbit on August 15, 2002 after the launch of Jason-1 on December 7, 2001. Topex/Poseiden was decommissioned on October 9, 2005. The Topex/Poseiden data products were generated with its sole Brown-model based retracker (herein after referred to as the Ocean retracker) (Rodríguez and Martin, 1994) for all different types of surfaces. In the original Topex/Poseiden data products, the geographic coordinates were provided for the 1 Hz elevation measurements. In this study, we utilized the data products created by RADS for the evaluation. The distance between two adjacent 1-Hz measurements along satellite track is about 6 km. Jason-1 was shifted to the interleaved orbit on February 10, 2009, after the launch of Jason-2 on June 20, 2008. Jason-1 stayed on the interleaved orbit for 3 years until May 7, 2012 when it was adjusted to a geodetic orbit. It was finally decommissioned on July 1, 2013. Jason-2 was transferred to the interleaved orbit on October 17, 2016, after the launch of Jason-3 on January 17, 2016. It maintained the interleaved orbit for 8 months and then transferred to a geodetic orbit on July 10, 2017. It was decommissioned on October 1, 2019. Jason-3 now operates on the nominal orbit and will continue until the planned launch of Sentinel-6 Michael Freilich ~~Jason-CS/Sentinel-6~~ in 2020. Two retrackers have been used by all three missions to generate elevation measurements: the Brown-model based MLE4 retracker for ocean surfaces and the model-free Ice retracker (similar to OCOG/Ice1 retracker) for non-ocean surfaces (see the Jason-1, 2 &3 Products Handbook for details). Another Brown-model based retracker MLE3 has also been adopted for Jason-2 and Jason-3. Due to its apparent inferior performance in comparison with MLE4 (Thibaut et al., 2010;Vu et al., 2018), it is not included for our evaluation. All these three radar altimetry missions provide elevation measurements at a rate of 20 Hz. The ground distance between two adjacent measurements is about 350 m. We obtained the altimetry data products of these three missions from AVISO+ for the evaluation.

The *Sentinel-3* mission consists of two identical satellites, the Sentinel-3A and Sentinel-3B, which were launched on February 16, 2016 and April 25, 2018, respectively. The ground tracks of Sentinel-3B fall exactly in the middle of the

300    ground tracks of Sentinel-3A. In other words, the Sentinel-3B is operated on an interleaved orbit, in parallel with the Sentinel-3A on the nominal orbit. The two orbits have the same 27 days repeat cycle and collect elevation measurements along their ground tracks between 81.35°N and 81.35°S latitudes (Donlon et al., 2012). Both satellites carry a Synthetic Aperture Radar altimeter instrument (SRAL) for the elevation measurements. The SRAL works primarily on the Synthetic Aperture Radar (SAR) mode with the Low Resolution Mode (LRM) as a back-up (Sentinel-3-Team, 2017). Four retrackers

305    are used in the SAR mode to produce elevation measurements, including SAR Altimetry Mode Studies and Applications -3 (SAMOSA-32), Offset Center of Gravity (OCOG), Sea-Ice, and Ice-Sheet (MSSL/UCL/CLS, 2019) (Shu et al., 2020). The OCOG (also known as Ice1) is a model-free retracker developed by Wingham (1986). The other three are model-based fully-analytic or semi-analytic retrackers (Shu et al., 2020). Due to the high rate of missing data (Shu et al., 2020), the Sea-Ice retracker is not included for the evaluation in this study. The elevation measurements are provided at a rate of 20 Hz. The

310    interval between two adjacent measurements along the satellite track is about 300 m (Sentinel-3-Team, 2017). We obtained the Sentinel-3 altimetry data from the ESA Copernicus Open Access Hub (https://scihub.copernicus.eu/) for the evaluation.

In this study, the altimetry data collected by each mission in geodetic phase (or drifting phase) are not included in the evaluation. In the geodetic phase, the drifting ground tracks do not generate frequent observations for a specific lake to form time series of water level measurements. In this study, for all the completed missions, only the data collected in their exact

315    repeat phase are used for the evaluation. For instance, the data collected in Phase ERM were used for GeoSat and the data collected in Phase R, C and G were used for ERS-1. In the "Extension Phase" of ENVISatENVISAT mission and in the intermittent phases of Topex/Poseiden, Jason-1 and Jason-2 missions, the satellites all operated on exact repeat orbit. Therefore, the data collected in these phases were also included in the evaluation. For the two currently operational missions Sentinel-3 and Jason-3, the observations for longer than a full year (including winter and summer) are used for the

320    evaluation, namely, Jason-3 data between February 2016 and March 2018 and Sentinel-3 data between June 2016 and September 2017.

In addition to the altimeter instrument, most of the eleven satellite missions (except for GeoSat) also carried a passive microwave radiometer (MWR) to simultaneously measure the brightness temperature (referred to as $T_B$) of Earth's surface. The microwave bands adopted by each mission are listed in Table 2.

325    **4 Lake water level determination and accuracy evaluation methods**

The method used to determine lake water level from satellite radar altimetry in this study consists of three technical data processing steps. First, the surface elevation measurements are retrieved from altimetry data products of the eleven satellite missions for the twelve case study lakes, and the most recent release —e of the altimetry data products with the up-to-date geophysical corrections have been used. Second, the spurious surface elevation measurements are filtered out through

330    statistical analysis, and the remaining valid surface elevation measurements within a lake are statistically aggregated to determine lake water level at different time points. Third, the ice-cover condition is examined using the simultaneous $T_B$

measurements from the MWR instruments, and those lake water level estimates during the ice-covered period are excluded in the subsequent accuracy evaluations. To evaluate the performance of each satellite altimeter and its retrackers, three accuracy measures, including the Pearson's correlation coefficient *r*, the bias and the *RMSE*, have been calculated by
335 comparing the radar altimetry derived lake water level estimates with the corresponding *gauge* measurements.

## 4.1 Retrieval of lake surface elevation measurements

Following Crétaux *et al.* (2017), the surface elevation is determined for each satellite radar altimetry mission according to Equation 1:

$$h_{retrk} = H - R_{retrk} - (\Delta R_{iono} + \Delta R_{wet} + \Delta R_{dry} + \Delta R_{solidEarth} + \Delta R_{pole}) - Geoid \qquad (1)$$

340 where $h_{retrk}$ is the surface elevation generated by a retracker, $H$ is the height of satellite orbit, $R_{retrk}$ is the range between the satellite and the nadir Earth's surface generated by a retracker, $\Delta R_{iono}$, $\Delta R_{wet}$ and $\Delta R_{dry}$ compensate the delay of radar pulse due to the ionosphere, the wet troposphere and the dry troposphere, respectively, $\Delta R_{solidEarth}$ and $\Delta R_{pole}$ are for solid Earth tide correction and pole tide correction, $Geoid$ converts the reference surface from ellipsoid to geoid (orthometric height). In this study, the geoid model EGM2008 (Pavlis et al., 2012) is adopted.

345 Due to the variable nature of Earth's atmosphere, the three atmospheric components ($\Delta R_{iono}$, $\Delta R_{wet}$ and $\Delta R_{dry}$) have significant influences on the accuracy of altimetry measurements (Fernandes et al., 2014;Fernandes and Lázaro, 2016;Crétaux et al., 2009;Scharroo and Smith, 2010). Many global atmospheric models have been used to quantify the biases induced by the three atmospheric components at different locations and times. For the ionospheric correction ($\Delta R_{iono}$), it has been recommended to use the NIC09 (New Ionosphere Climatology) model for the radar altimetry
350 measurements acquired before September 1998 (Scharroo and Smith, 2010) and to use the GIM (Global Ionosphere Map) model for the measurements acquired after that time (Iijima et al., 1999). For the dry and the wet tropospheric corrections ($\Delta R_{dry}$ and $\Delta R_{wet}$), the three most commonly used atmospheric models are produced by the European Centre for Medium-Range Weather Forecasts (ECMWF) and the National Centers for Environmental Prediction (NCEP). Those include the ECMWF model (Miller et al., 2010), the ECMWF Re-Analysis Interim (ERA) model (Dee et al., 2011), and the NCEP
355 model (Caplan et al., 1997). The magnitude of the dry and the wet tropospheric corrections depends linearly on the height of the surface over which the altimetry measurement is made. The higher the surface elevation, the smaller the magnitude of the dry and the wet tropospheric correction terms. The difference between the dry tropospheric corrections computed at the sea surface with an elevation of 0 m and at the surface with an elevation of 5000 m could be as high as 1 m (Fernandes et al., 2014). Fernanders and Lázaro (2016) also developed a new algorithm to improve the wet tropospheric corrections that can
360 be applied to different radar altimetry missions. In this study, since we focus mainly on the official data products generated by each satellite mission~~For all the altimetry data products adopted in this study~~, we adopted the dry and the wet tropospheric corrections that were contained in the official data products and were computed with the height of the surface

where the altimetry measurements were taken. Table 3 lists the version of each altimetry data product and the models of the three atmospheric corrections utilized in this study.

## 4.2 Statistical determination of lake water levels

The twelve case lakes in this study were all overpassed by the eleven satellite radar altimetry missions. The number of each mission's ground tracks on these lakes is determined by the size of lake and the satellite orbit. The large lakes (Lake Superior) usually have multiple ground tracks for each mission, while the small lakes (e.g. Lokka) may have only one ground track for a satellite mission. For a large lake (e.g. the Great Lakes), strong wind, big wave, diurnal tide, geoid undulation, and other factors may significantly influence lake water level at different locations in the lake. The *in-situ* water level measurements from a gauge station may not reflect the actual water level of those ground tracks far away from the gauge station. Thus, the overall *RMSE* of the altimetry-derived estimates will increase when altimetry observations from distant ground tracks are included for the evaluation (Birkett, 1995). To minimize the possible influence of wind, waves, tide and other environmental factors for an objective comparison between different satellite missions, we thus select the ground track nearest to the gauge station and exclude distant ground tracks in the performance evaluationFor lakes with more than one ground tracks, we selected the one near the gauge station for the evaluation, as listed in Table 4. CryoSat-2 uses a geodetic orbit (long-term repeat orbit). It is difficult to form a frequent time series of co-located water level estimates for the evaluation. Although a time series of water level estimates from CryoSat-2 observations can be derived for a large lake by including many different ground tracks, this will inevitably introduce uncertainties to the evaluation due to the factors as explained above. This is the reason that we did not include the Cryosat-2 data and the data collected by other satellite missions during their geodetic phases or drifting phases.

The total number of completed cycles for each mission depends on its operational lifetime and the temporal length of a repeat cycle. For a mission with long lifetime and short repeat cycle, the overpass number could be much higher. As listed in Table 4, Topex/Poseiden has the highest number of complete cycles (333 in the nominal phase and 111 in the intermittent phase). In each repeat cycle, there is one satellite overpass along the selected ground track for each mission.

Spurious elevation measurements could be generated when the satellite ground track passes over lake islands or when it is close to lake shore. Particularly, the complex surrounding topography could have considerable influences on the elevation measurements over very small lakes (width less than 2 km) or over rivers, when considering the tracking modes (e.g. the open/close loop of Sentinel-3 and Jason-3) and the receiving window sizes (e.g. the three different window sizes of ENVISAT) of the radar altimeter (Jiang et al., 2020;Biancamaria et al., 2018). The smallest case study lake in our evaluation is Reservoir Lokka in Finland with a surface area of about 500 km$^2$. For each mission, the ground track over the lake is at least 10 km long. In this study, two steps were adopted to minimize the influences. First, for each satellite overpass during the exact repeating phase, we first extracted the surface elevation measurements along a ground track falling within lakes using lake polygons from the GLWD. Considering the footprint size of radar pulses over relatively homogeneous surface (usually 1 – 2 km) and the seasonal fluctuation of lake surface area, only elevation measurements over 2 km away from the

polygon boundary are selected. Then, the extracted elevation measurements along each ground track were combined to form a surface elevation profile, which was examined to filter out the spurious measurements with the robust Median-Absolute-Deviation (*MAD*) statistic (Shu et al., 2018;Liu et al., 2012;Shu et al., 2020). The spurious measurements deviate significantly from the other measurements of the lake surface elevation profile. The spurious measurements could possibly be induced by the contamination of land surface when the satellite ground track passes through lake islands or when it is close to lake shore. The *MAD* method calculates a statistic score for each measurement of the surface elevation profile to indicates its deviation from the rest of the measurements. The higher the score the stronger deviation is. The measurements with a score value larger than or equal to three are excluded. The median of the remaining elevation measurements along the track is then used as the estimate of the lake water level on the day of each satellite overpass. Finally, the time series of water level estimates were evaluated through comparing with the concurrent gauge measurements.

### 4.3 Identification of lake level estimates affected by ice cover

Lakes located in high latitude in this study are more frequently overpassed by satellite missions, but the ice cover on these lakes in the winter season may introduce significant errors to the elevation measurements of satellite altimetry missions. It has been demonstrated that the lake ice cover in winter could have strong influences on the radar altimetry signal pulse, resulting in lower elevation measurements than the real lake surface elevation (Birkett and Beckley, 2010;Ziyad et al., 2020). The mechanism on how lake ice deforms the radar Sentinel-3 altimetry signal pulse and fails the official waveform retracking algorithms has been investigated in (Shu et al., 2020). Shu *et al*. (2020) also developed a non-official correction algorithm to accurately retrieve the water-equivalent lake levels in ice-covered condition from Sentinel-3 altimetry observations. Since the official retrackers of all the satellite altimetry missions (not only Sentinel-3) are not designed to handle the ice-cover on lakes, we identified and excluded the measurements obtained in the ice-covered condition in order to have a fair comparison between different altimetry missions.

In this study, we followed the method in (Shu et al., 2020) to examine the ice cover condition for all satellite radar altimetry missions over the case study lakes. Namely, we examine the temporal variations of brightness temperature ($T_B$) over lake surface to detect the lake ice cover. Similar to the preprocessingpre-processing of radar altimetry surface elevation measurements, we first filter the simultaneous microwave $T_B$ measurement profile along the track over a lake. Then, all the remaining valid microwave $T_B$ measurements were averaged to represent the temperature for the day of each satellite overpass. The time series curve of $T_B$ was then analyzedanalysed to determine the dates of ice-on and ice-off for each winter, indicated by the sudden increase and rapid decrease of $T_B$ on the curve. Those radar altimetry measurements collected in the ice-covered condition were identified and then excluded from the subsequent evaluations.

## 4.4 Accuracy measures for the performance evaluation

The performance of a satellite altimetry mission and its retrackers were evaluated in terms of three accuracy measures as in (Shu et al., 2020), including the Pearson's correlation coefficient ($r$), the bias ($Bias$) and the root mean square error ($RMSE$). The $Bias$ and the $RMSE$ were computed as below.

$$Bias = \frac{1}{n}\sum_{i=0}^{n}(H_{retrk}^{i} - H_{gauge}^{i}) \tag{2}$$

$$RMSE = \sqrt{\frac{1}{n}\sum_{i=0}^{n}(H_{retrk}^{i} - H_{gauge}^{i} - Bias)^2} \tag{3}$$

where $n$ is the total number of a satellite mission's overpasses along the selected track on a lake, $i$ is the index of an overpass, $H_{retrk}^{i}$ is the altimetry-derived lake level estimate for satellite overpass $i$ given by a specific retracker, $H_{gauge}^{i}$ is the concurrent gauge measurement at the time of overpass $i$.

These three accuracy measures are computed for each retracker of each mission over each lake. The $Bias$ represents the systematic (positive or negative) difference between the series of altimetry-derived estimates and the gauge measurements. If both are referenced to the same vertical datum (e.g. EGM2008), then the smaller the $Bias$, the closer altimetry-derived estimates to the real lake water level. Since the datums of the altimetry-derived water levels and the gauge measurements were consistent only for the Great Lakes as mentioned in Section 2.2, we compared and evaluated the biases of all the retrackers of the eleven missions for these five lakes. The Pearson correlation coefficient $r$ indicates each retracker's capability in depicting lake water level temporal variation. A high $r$ value shows that the retracker captures the lake water level variation very well. Note that the correlation coefficient $r$ is not affected by systematic errors/biases or vertical datum differences. In our evaluation, the $RMSE$ is calculated after the $Bias$ of each retracker over each lake was removed (Shu et al., 2020). The $RMSE$, hence, represents the relative accuracy (precision) of the altimetry-derived lake level estimates. By removing the $Bias$, the inconsistency between the vertical datums of the altimetry-derived water levels and the *gauge* measurements would not affect $RMSE$ values, making all the retrackers over the twelve lakes comparable to each other in terms of $RMSE$ value.

## 5 Results

### 5.1 Radar altimetry derived Lake water level estimates

Fig. 3 shows the time series of $T_B$ and altimetry-derived water levels over Great Slave Lake collected by ~~ENVISat~~ENVISAT, Jason-2 and Sentinel-3 in the winters of 2003/2004, 2011/2012, and 2016/2017, respectively. The ice-covered duration is determined by the sudden increase and the decrease of $T_B$, as indicated by the vertical dash lines in Fig. 3a, 3b and 3c. The similar temporal variation of $T_B$ was also observed for other satellite missions over other lakes when they were covered by ice. As shown in Fig. 3d, 3e and 3f, the lake water level estimates during the ice-covered periods deviate significantly from

the gauge measurements, while during the ice-free seasons the lake water level estimates correlate very well with the gauge measurements.

Table 5 summarizes the number of lake level estimates during ice-free (open water) and ice-covered seasons over each lake for each retracker of the eleven missions. For some satellite missions, the number of valid lake water level estimates over a certain lake during ice-free season was too small to perform an evaluation. For example, the number of GeoSat estimates over Lake Inarijarvi, Lake Lokka, Lake Oulujarvi and Lake Cedar are all less than three. Therefore, the evaluation of GeoSat over these lakes was not conducted. As shown in Table 5, the total number of lake water level estimates (~sum of the ice-covered number and the ice-free number) for some satellite missions, such as GeoSat and GFO, are considerably smaller than the number of completed orbit cycles, due to satellite data loss. The reasons for satellite data loss could be the malfunction of the sensor, the maneuver of the satellite during the phase transition, the failure of the retracker to reach convergence when processing complex waveforms (e.g., multi peaks) from inhomogeneous reflecting surfaces in the altimeter footprint, saturation of the sensor over very bright targets, or the rapid changes of the topography that are larger than the size of tracking window causing tracking losses (Biancamaria et al., 2017).

We calculated the data loss rate of lake level estimates over each lake for each retracker of the eleven missions. For each satellite repeat cycle, there is a satellite overpass along the selected ground track on each lake and there is supposed to be a lake water level estimate if valid surface elevation measurements exist. In this study, the data loss rate of lake level estimates (not the data loss rate of elevation measurements) is calculated through dividing the total number of water level estimates (sum of the ice-covered number and the ice-free number) by the total number of repeat cycles. As shown in Table 6, GeoSat has very high data loss rate for almost all the lakes. The average data loss rate is 65.42%. There are seven lakes with a loss rate higher than 70%. Particularly, the data loss rate over small lakes is much higher than that for large lakes. The highest data loss rate is 98.51% over Lake Cedar. The high data loss rate could be partly due to GeoSat low sampling rate (1Hz). The other possible reason is the failure of lock-on to return pulse during transition from land to water, as documented in Section 5 of GeoSat_user_handbook (https://www.nodc.noaa.gov/archive/arc0024/0053056/2.2/about/ userhandbook.pdf) (Cheney, 1997). Similarly, GFO also has very high data loss rate for small lakes. The highest data loss rate is 80% over Lake Cedar. The high data loss rates of GeoSat and GFO hamper their usefulness for retrieving lake water levels. In contrast, SARAL and Sentinel-3 have a very low data loss rate over both large lakes and small lakes. For ERS-2 and ENVISatENVISAT, the data loss rates over small lakes are slightly higher than that over large lakes. Another interesting observation is that on average the model-based retrackers have a relatively higher data loss rate than model-free retrackers for all missions. For example, the data loss rates of MLE4 retracker of Jason-1, -2 and -3 missions are 21.48%, 16.45% and 15.7%, about twice as high as the loss rates of the Ice retracker of these three missions (12.8%, 6.61% and 6.20%). It suggests that the model-free retrackers are more reliable than model-based retrackers for producing continuous lake water level estimates, confirming the observations of Frappart *et al*. (2006) and Sulistioadi *et al.* (2015).

## 5.2 The *Biases* of altimetry-derived lake water level estimates

We construct a long-term series of lake water levels for each of the twelve lakes using the altimetry-derived estimates during ice-free seasons. Fig. 4a shows the lake water level time series over Great Slave Lake. For many satellite missions, there are more than one water level time series from different retrackers. Fig. 4a displays only the water level time series produced by
490 the retracker of each mission that has the lowest data loss rate in Table 6. For example, the water level time series produced by Jason-1 Ice retracker, rather than MLE4 retracker, were displayed.

Clearly, *biases* exist between the altimetry-derived estimates and the gauge measurements for all missions. The magnitude of the *biases* varies among the missions. If altimetry-derived water levels and gauge data are both reference to the same vertical datum, Tthe small magnitude of bias indicates that the absolute values of altimetry-derived lake water level are close to the
495 ground truth represented by gauge measurements. As shown in Fig. 4a, the time series of T/P water level estimates (given by Ocean retracker) have the least difference to the gauge data on Great Slave Lake in absolute values, while the time series of ERS-2 estimates (produced by Ice1 retracker) have the largest absolute difference from the gauge measurements. As shown in Fig. 4b, after removing the *biases*, the altimetry-derived estimates match the gauge measurements well for most of the missions over Great Slave Lake.

500 The *bias* value for each retracker of the eleven missions over the twelve lakes are reported in Table 7. Since only the Great Lakes' gauge measurements are referenced to the same vertical datum as altimetry-derived lake water levels, we will then focus our discussion of the *bias* on these five Great Lakes. For a specific lake (e.g. Lake Erie) the different missions and different retrackers of the same mission could have very different magnitudes of *biases*. The mean bias with respect to gauge data is calculated for each retracker by averaging the *biases* over the five Great Lakes. As shown in Table 7, the retrackers
505 with a mean *bias* less than 10 cm include the Ocean retracker of Topex/Poseiden mission, the MLE4 retracker of Jason-1, -2 and -3 missions, and the Ice-Sheet and SAMOSA3 SAMOSA-2 retracker of Sentinel-3 mission. The mean *Bias* of Jason-3 MLE 4 retracker is less than 1 cm. Note that all those low bias retrackers are model-based. Actually, for all missions with multiple retrackers, the model-based retrackers outperforms the model-free retracker in terms of mean *bias* over the Great Lakes.

## 5.3 The performance of radar altimetry missions in capturing lake water level dynamics

510 The Pearson's correlation coefficient *r* was calculated for all the retrackers of each mission over every lake that has more than three lake water level estimates. A high correlation coefficient of the lake water level estimates from a retracker with *gauge* measurements indicates a strong capability of the retracker in reconstructing the temporal variation of lake water levels. As shown in Table 8, all the retrackers of the eleven missions, except for ERS-1 Sea-Ice retracker, have a good
515 performance on large lakes (e.g. the Great Lakes). In contrast, many retrackers give a *r* value less than 0.7 over small lakes. ERS-1 Ocean retracker gives the lowest *r* value of 0.07 over Lake Oulujarvi.

The performances of SARAL and Sentinel-3 missions in capturing the lake water level dynamics are outstanding. Almost all their retrackers produce a very high *r* value over both large and small lakes. Their stronger capabilities than other satellite radar missions of retrieving water levels for small waterbodies were previously reported in (Bogning et al., 2018;Normandin
520  et al., 2018). The Sentinel-3 Ice1 retracker gives the highest mean *r* value (0.96) across the twelve lakes. In contrast, ERS-1 Sea-Ice retracker has very poor performance over almost all the lakes, even on very large lakes, resulting in the lowest mean r value of 0.50.

As indicated in Table 8, for all the missions the model-free retrackers (except for ERS-1 Sea-Ice retracker) outperform the model-based retrackers in depicting water level variations over small lakes. The model-free retrackers, including the Ice1 (or
525  OCOG) retracker of ERS-1, ERS-2, ~~ENVISat~~ENVISAT, SARAL and Sentinel-3 missions, and the Ice retracker of Jason-1, -2 and -3 missions, all yield higher *r* values than model-based retrackers of the same missions over small lakes. The performance contrast between model-free and model-based retrackers is particularly conspicuous over Lake Oulujarvi and Lake Vanern. Fig. 5 shows the scatterplots produced by the model-free retrackers of ERS-1, Jason-2 and Sentinel-3 over the lakes Oulujarvi, Vanern and Erie. Fig. 6 shows the corresponding scatterplots produced by the model-based retrackers (ERS-
530  1 Ocean, Jason-2 MLE4 and Sentinel-3 ~~SAMOSA3~~SAMOSA-2) of the same missions over the three lakes. Apparently, the estimates given by model-free retrackers correlate very well with gauge measurements for all three missions over the three lakes. The correlation is higher on large lakes (e.g. Lake Erie) than on small lakes (e.g. Lake Oulujarvi). In contrast, no clear correlation can be observed between the water level estimates from ERS-1 Ocean retracker and Jason-2 MLE4 retracker and gauge measurements on Lake Oulujarvi. The correlation of Jason-2 MLE4 retracker estimates with gauge measurements on
535  Lake Vanern is very low. It suggests that in comparison with the model-based retrackers, the model-free retrackers (OCOG/Ice1/Ice) are less affected by the contamination of land surface surrounding small lakes.

## 5.4 Overall precision of altimetry-derived lake water level estimates from different missions

As introduced in Section 4.4, the *RMSE* was computed for each retracker after removing the bias, which contains the vertical datum difference between satellite and ground measurements and systematic error between the gauge station and retrackers.
540  Such calculated *RMSE* represents the precision of altimetry-derived lake water level estimates as compared with gauge measurements. A small *RMSE* of a retracker means a small random error, hence a high precision of the retracker in retrieving lake water levels. The *RMSE* values for all retrackers of the eleven missions over the twelve lakes are listed in Table 9. Similar to the pattern that we observed for the correlation coefficient r, the *RMSE* values for large lakes are significantly smaller than those for small lakes. Most retrackers of the eleven missions have a *RMSE* less than 10 cm for large lakes. The
545  *RMSE*s for small lakes, however, may exceed 30 cm. Among all retrackers and all missions, SARAL Ice2 retracker givers the lowest *RMSE* of (1.92 cm) over Lake Ontario, while GFO produces the highest *RMSE* of 132.81 cm over Lake Oulujarvi. Again, it reflects the adverse influences of land surface on the accuracy of satellite altimeters in the retrieval of lake water levels for small lakes.

As compared to other missions, Sentinel-3 and SARAL have clearly better measurement precision in terms of *RMSE* over
550  small lakes, such as Lake Inarijarvi, Lokka and Oulujarvi, which are largely due to the smaller footprint of the altimeters
onboard these two missions. Most retrackers of these two missions yielded a *RMSE* less than 30 cm over the three lakes. In
contrast, the *RMSE*s of ERS-1 retrackers over these three lakes are mostly higher than 50 cm. The mean *RMSE*s of the three
Sentinel-3 retrackers (7.31 cm for Ice-Sheet, 6.08 cm for OCOG and 6.57 cm for SAMOSA-2~~3~~) are much smaller than other
missions. The mean *RMSE*s of the SARAL retrackers (7.89 cm for Ice1, 7.30 cm for Ice2, 8.85 cm for Sea-Ice and 10.46 cm
555  for Ocean retracker) are slightly higher than Sentinel-3 retrackers.

For the same mission, model-free retrackers often have lower *RMSE*s than the model-based retrackers. For example, the
average *RMSE*s across the twelve lakes are 14.76 cm for ERS-1 Ice1, 11.28 cm for Jason-1 Ice, 7.74 cm for
~~ENVISat~~ENVISAT Ice1, 8.18 cm for Jason-2 Ice and 8.03 cm for Jason-3 Ice retracker. In contrast, the average *RMSE*s are
35.17 cm for ERS-1 Ocean, 18.68 cm for Jason-1 MLE4, 14.66 cm for ~~ENVISat~~ENVISAT Ocean, 19.22 cm for Jason-2
560  MLE4 and 17.15 cm for Jason-3 MLE4 retracker. The mean *RMSE* of the model-based retrackers is approximately twice as
large as that of the model-free retrackers. The performance contrast in terms of *RMSE* between the two types of retrackers is
striking for small lakes. On Lake Oulujarvi, the *RMSE*s for the Ice retracker of Jason-1, -2 and -3 missions are 17.42 cm,
17.16 cm and 24.65 cm. But, the *RMSE*s of the MLE retracker of these three missions are 124.98 cm, 99.91 cm and 110.32
cm, 5 – 6 times higher than the model-free retrackers. Again, it highlights the fact that model-free retrackers are more precise
565  choices for the retrieval of water levels for small lakes. For large lakes, both types of retrackers have similar performance in
lake level estimates. Therefore, the selection of either model-free or model-based retracker does not make much difference in
the precision of water level estimates for large lakes.

**6 Discussion**

Among the eleven satellite radar altimetry missions, eight of them have more than one retrackers to measure the Earth's
570  surface elevation. It should be noted that none of these retrackers were dedicated to the surface elevation measurements of
inland lakes. Our evaluation intention is to identify which retrackers have relatively better performance. As shown in Tables
6, 8 and 9, all the retrackers of the same mission have similarly good performance for large lakes (e.g. the Great Lakes) in
terms of the data loss rate, the correlation coefficient *r* and *RMSE*. In other words, any of the retrackers for the same mission
(except for the ERS-1 Sea-Ice retracker) could be used to retrieve water levels for a large lake. However, for small lakes, the
575  model-free retrackers, such as the Ice1 (OCOG) retracker of ERS-1, ERS-2, ~~ENVISat~~ENVISAT, and SARAL, and the Ice
retracker of Jason-1, -2 and -3, are clearly better choices than the model-based retrackers, such as the Ocean retracker of
ERS-1, ERS-2, ~~ENVISat~~ENVISAT, and SARAL, and the MLE4 retracker of Jason-1, -2 and -3, or the non-model based
retracker Sea-Ice. Our evaluation result is contrary to Sulistioadi (2015), who found comparable performances between Sea
Ice and OCOG retrackers over a couple of small lakes (Lake Matano and Lake Towuti in Indonesia) using
580  ~~ENVISat~~ENVISAT data. In previous study, Frappart (2006) concluded that the model-free Ice1 retracker was the best

among the four ~~ENVISat~~ENVISAT retrackers in the retrieving lake water levels. Our evaluation results consistently demonstrate that for all radar altimetry missions model-free retrackers tend to have high correlation coefficients, lower data loss rates and *RMSE*s than the model-based retrackers over small lakes. The model-free retrackers are therefore recommended for the retrieval of water levels over small lakes.

585 It is evident that the performance of the satellite radar altimetry missions has been improving with the time, as observed from Tables 6, 8 and 9. In general, the new generation of radar altimetry mission performs better than historical missions. The data loss rate decreases from 65.42% for the first-generation mission of GeoSat to 2.32% for the currently operational Sentinel-3 mission. The mean *RMSE* decreases from 35.17 cm of the early ERS-1 mission to 6.~~47~~08 cm of the current Sentinel-3 mission. Among the eleven missions, the most recent Sentinel-3 mission has the best performance. All three retrackers

590 (particularly the OCOG retracker) produced the lowest mean *RMSE*s and the lowest mean data loss rate among all historical and currently operational missions. The SAMOSA-2 retracker has slightly higher *RMSE* and clearly lower bias than OCOG retracker. The reason is that the SAR altimeter onboard Sentinel-3 increases the along-track sampling resolution (~300 m) and maximizes the information retrieval over variable terrain surfaces (Donlon et al., 2012).

Following Sentinel-3, SARAL gave the second-best performance among these missions. The Ice1 retracker of SARAL

595 performed well for both small lakes and large lakes. For the period between February 2013 and June 2016, the SARAL Ice1 retracker provided the best retrieval of water levels for the overpassed lakes, due to its smaller footprint and larger bandwidth owing to the use of Ka-band (Bonnefond et al., 2018). Between February 2002 and April 2012, the Ice1 retracker of ~~ENVISat~~ENVISAT mission provided very accurate retrieval of lake levels. Overall, the ~~ENVISat~~ENVISAT Ice1 retracker gave slightly better results than the Ice retracker of Jason-1 and Jason-2 missions. However, since the repeat cycle of

600 ~~ENVISat~~ENVISAT is 35 days and the data loss rate of ~~ENVISat~~ENVISAT Ice1 retracker is almost twice as high as that of Jason-1 and Jason-2 missions, the two Jason missions (with a repeat cycle of 10 days) provided temporally more frequent and continuous estimates of lake water levels than ~~ENVISat~~ENVISAT. It should be noted that Jason-1 and Jason-2 cover only the Earth's surface between 66°N and 66°S latitudes. For lakes located at high latitude polar regions, ~~ENVISat~~ENVISAT is the best alternative option during its operational time.

605 GFO has a much higher data loss rate than other contemporary missions. For the lakes overpassed by GFO, ERS-2 and Topex/Poseiden in the same period of time, GFO is the least desirable choice. For the period from 1991 to 2001, ERS-1 and ERS-2 are better choices for small lakes than Topex/Poseiden. But for large lakes, Topex/Poseiden should be adopted since it has much more frequent overpasses than ERS-1 and ERS-2 satellites, although comparable accuracy for lake level estimates. GeoSat exhibited a good performance for large lakes (e.g. the Great Lakes). Even though it has an extremely high

610 data loss rate for almost all the twelve lakes, the water level estimates given by GeoSat are still valuable since it was sole satellite radar altimetry mission between 1985 and 1989.

To construct a long-term time series of lake water level for an ungauged lake, one critical step is to determine a reference mission to tie all satellite missions together by compensating the biases between them. A reference mission should meet two requirements. First, the reference mission should be able to provide precise lake level estimates, at least comparable with

615  other missions. Second, the reference mission should have a long operational time period so that it has temporal overlaps with many other missions. Both Sentinel-3 and SARAL meet the first requirement, due to their high performance for both large and small lakes. However, they have a relatively short temporal overlap with other missions and do not satisfy the second requirement. Among eleven radar altimetry missions, there are four missions that have a nominal operational time over 10 years (the geodetic phase not counted), including Topex/Poseiden, Jason-1, ~~ENVISat~~ENVISAT and Jason-2.

620  Topex/Poseiden does not meet the first requirement well since its performance is apparently inferior to Jason-1, ~~ENVISat~~ENVISAT and Jason-2 in terms of the *r*, *RMSE* and the data loss rate. Despite its long data duration, ~~ENVISat~~ENVISAT has higher data loss rate and longer repeat cycle, hence less frequent water level estimates than Jason-1 and Jason-2 missions, which reduces the chance of concurrent overpasses of ~~ENVISat~~ENVISAT with other missions over the same lake. In comparison, Jason-2 is a better choice as the reference mission than Jason-1. First, the Ice retracker of

625  Jason-2 has much smaller *RMSE* and lower data loss rate than Jason-1, as shown in Table 6 and 9. The Jason-2 Ice retracker's performance ($r = 0.93$, $RMSE = 8.18$ cm) in retrieving lake water levels is close to the best performance retracker-Sentinel-3 OCOG ($r = 0.96$, $RMSE = 6.47$ cm). Second, Jason-2 temporally overlapped with 7 other missions, including ERS-2, GFO, Jason-1, ~~ENVISat~~ENVISAT, Saral, Jason-3 and Sentinel-3. Jason-1 has 6 overlaping missions as shown in Table 2. Third, Jason-2 has a short repeat cycle of 10 days, hence the better chance to find concurrent overpasses

630  with other missions over the same lake. Moreover, for the four Topex/Poseiden–Jason satellites, the predecessor and the successor satellites measure the same location almost the same time (separated by 60 – 70 seconds) during their tandem phases. This allows for the accurate estimation of the inter-mission biases between them over the large lakes around the world. For example, based on the measurements during the tandem phases over the five Great Lakes, the estimated biases (with the successor satellite as the benchmark) are 0.48±4.48 cm for Topex/Poseiden and Jason-1, 19.56±5.38 cm for Jason-

635  1 and Jason-2, and -20.47±0.16 cm for Jason-2 and Jason-3. Using Jason-2 as the initial reference, we are able to form a consistent Topex/Poseidon-Jason series of water level estimates that overlaps with all other radar altimetry missions (except for GeoSat). This consistent series of water level estimates can be further used as the reference for other missions to estimate the biases between them, then construct the long-term time series of water level records at global scale. As discussed above, the model-free retrackers outperform the model-based retrackers over small lakes. For the purpose of constructing consistent

640  long-term time series of lake water levels, it is better to use the same model-free retracker (e.g. OCOG/Ice/Ice1) for both large and small lakes to avoid possible inter-mission retracker-induced biases.

When a lake was visited by more than one satellite missions on the same day, the best~~ ~~ water level estimate among the overlapping missions should be selected to form a long-term series of records, in terms of ~~the~~ the performance (*r* and *RMSE*) of the missions~~.~~. The water level estimates from the satellite mission with higher *r* value and lower *RMSE* should be used. For

645  the period before 2002, the order of selection priority should be ERS-2, ERS-1 and Topex/Poseidon. For the period of 2002 – 2013, the order of selection priority should be ~~ENVISat~~ENVISAT, Jason-2, Jason-1, ERS-2 and GFO. For the period 2013-2020, the order of selection priority should be Sentinel-3, SARAL, Jason-3 and Jason-2.

It should be noted that the lake sample size in this study is limited by two criteria. First, each case study lake must be overpassed by all the satellite missions evaluated in this study. Second, simultaneous *in-situ* gauge data are available for the sample lakes. After our thorough search, we identified the twelve lakes in this study that satisfy these two conditions. As compared to previous similar evaluation studies (as mentioned in the introduction), the twelve lakes still represent the largest sample size. More importantly, these lakes are located in different continents, latitudes and geographical environments. They include both natural lakes and reservoirs. These lakes have different sizes and winter ice conditions. They form a representative sample of the majority of inland lakes around the world. Nevertheless, we agree that it is even better if we have much larger sample size that satisfy the above conditions and we hope to include more sample lakes in our future research when their *in-situ* gauge data become available.

## 7 Conclusions

Thirteen satellite radar altimetry missions have been launched to measure the Earth's surface elevation since 1985. The satellite radar altimetry data collected by these missions have been widely utilized for retrieving lake water levels. Although some previous studies assessed some missions in retrieving lake water level, our knowledge and understanding are still limited as to the comparative advantages of different retrackers across different radar altimetry missions and the effective strategy of tying all missions together to reconstruct a long-term time series to support the investigation of lake water level dynamics. In this study, we made a comprehensive evaluation on the performances of the different retrackers of eleven missions using a consistent data processing procedure and algorithms over the same set of twelve case study lakes, where the *gauge* measurements are available. These twelve lakes are representative for different areal size, local climate and surrounding environment.

Among the eleven missions, the most recent mission Sentinel-3 gave the most accurate estimates, largely due to the adoption of new SAR altimetry technology. All three retrackers (particularly the OCOG retracker) of Sentinel-3 yielded very accurate lake level estimates for both large and small lakes. These SAR altimetry echoes can be coherently processed in the future to further reduce the along-track sampling resolution, which is called as Fully Focused SAR (FF-SAR) altimetry (Kleinherenbrink et al., 2020). This could significantly increase the accuracy of lake water level estimates and would be a worthy direction of future investigation. SARAL's performance is the second best in retrieving lake water levels, owing to the advantages of the Ka band. Its Ice1 retracker works for both large and small lakes too. ENVISatENVISAT Ice1 retracker is slightly better than the Ice retracker of Jason-1 and Jason-2 in terms of *r* and *RMSE*. However, Jason-1 and -2 can provide more consistent, frequent and continuous lake water level estimates due to their low data loss rates and short repeat cycle. Although ERS-1 and ERS-2 (e.g. the Ice1 retracker) had clearly better performance over small lakes than T/P between 1991 and 2005, Topex/Poseiden is still recommended for retrieving water levels for large lakes since it had much more frequent estimates than ERS-1 and ERS-2. Both GeoSat and GFO exhibited extremely high data loss rates of lake water level estimates. GFO can be replaced by several other contemporary missions, such as T/P, ERS-2, Jason-1 and

680 ~~ENVISat~~ENVISAT. However, GeoSat was the earliest sole mission in the 1980s, therefore still valuable for extending the time series of lake water level as early as possible.

In order to reconstruct long-term time series of lake water level, a reference mission need to be selected to tie all other missions together. The best strategy for constructing long-term lake water level records should be a two-step bias correction and normalization procedure. In the first step, use Jason-2 as the initial reference to estimate the systematic biases with

685 Topex/Poseidon, Jason-1 and Jason-3 and then normalize them to form a consistent Topex/Poseidon-Jason series. Then, use Topex/Poseidon-Jason series as the reference to estimate and remove systematic biases with other radar altimetry missions to construct consistent long-term lake water level series for ungauged lakes. We found that the model-free retrackers (Ice1/OCOG/Ice) evidently perform better than the model-based retrackers in terms of the *RMSE*, the Pearson's correlation coefficient *r* and the data loss rate. For the missions with more than one retrackers, the model-free retracker is recommended

690 in the construction of the long-term time series of lake water level, particularly, for small lakes. For different time periods, multiple missions may have overpassed the same lake on the same day. We have worked out the priority order to select the measurements among overlapping missions in three time periods to construct the best possible lake water level time series.

## Competing interests

695 The authors declare that they have no conflict of interests.

## Author contribution

**Song Shu**: Conceptualization, Methodology, Software, Formal analysis, Writing - original draft. **Hongxing Liu:** Methodology, Supervision, Writing - review & editing. **Richard A. Beck**: Resources, Writing - review & editing. **Frédéric**

700 **Frappart:** Validation, Writing - review & editing. **Johanna Korhonen:** Validation, Writing - review & editing. **Minxuan Lan:** Data curation, Writing - review & editing. **Min Xu:** Writing - review & editing. **Bo Yang:** Writing - review & editing. **Yan Huang:** Writing - review & editing.

## Acknowledgements

705 The authors would like to thank the two anonymous journal reviewers for their constructive and insightful comments which help improve the quality of this manuscript.

## References

Adrian, R., O'Reilly, C. M., Zagarese, H., Baines, S. B., Hessen, D. O., Keller, W., Livingstone, D. M., Sommaruga, R., Straile, D., and Van Donk, E.: Lakes as sentinels of climate change, Limnology and oceanography, 54, 2283-2297, 2009.

710 Assel, R., and Wang, J.: Great Lakes Ice Cover Data - Ice Year 2017, in, edited by: Laboratory, N. G. L. E. R., 2017.

Barry, R., Finkelstein, J., Kilgus, C., Mooers, C. N. K., Needham, B., and Crawford, M.: Geosat follow-on satellite to supply ocean sciences data, Eos, Transactions American Geophysical Union, 76, 33-36, 10.1029/EO076i004p00033-02, 1995.

Berry, P. A. M., Garlick, J. D., Freeman, J. A., and Mathers, E. L.: Global inland water monitoring from multi-mission altimetry, Geophysical Research Letters, 32, https://doi.org/10.1029/2005GL022814, 2005.

715 Biancamaria, S., Frappart, F., Leleu, A. S., Marieu, V., Blumstein, D., Desjonquères, J.-D., Boy, F., Sottolichio, A., and Valle-Levinson, A.: Satellite radar altimetry water elevations performance over a 200m wide river: Evaluation over the Garonne River, Advances in Space Research, 59, 128-146, https://doi.org/10.1016/j.asr.2016.10.008, 2017.

Biancamaria, S., Schaedele, T., Blumstein, D., Frappart, F., Boy, F., Desjonqueres, J. D., Pottier, C., Blarel, F., and Nino, F.: Validation of Jason-3 tracking modes over French rivers, Remote Sensing of Environment, 209, 77-89, 10.1016/j.rse.2018.02.037, 2018.

720 Birkett, C., Reynolds, C., Beckley, B., and Doorn, B.: From Research to Operations: The USDA Global Reservoir and Lake Monitor, in: Coastal Altimetry, edited by: Vignudelli, S., Kostianoy, A. G., Cipollini, P., and Benveniste, J., Springer Berlin Heidelberg, Berlin, Heidelberg, 19-50, 2011.

Birkett, C. M.: The contribution of TOPEX/POSEIDON to the global monitoring of climatically sensitive lakes, Journal of Geophysical Research, 100, 25,179-"125,204", 1995.

725 Birkett, C. M., and Beckley, B.: Investigating the Performance of the Jason-2/OSTM Radar Altimeter over Lakes and Reservoirs, Marine Geodesy, 33, 204-238, 10.1080/01490419.2010.488983, 2010.

Bogning, S., Frappart, F., Blarel, F., Niño, F., Mahé, G., Bricquet, J.-P., Seyler, F., Onguéné, R., Etamé, J., and Paiz, M.-C.: Monitoring water levels and discharges using radar altimetry in an ungauged river basin: The case of the Ogooué, Remote Sensing, 10, 350, 2018.

Bonnefond, P., Verron, J., Aublanc, J., Babu, K. N., Bergé-Nguyen, M., Cancet, M., Chaudhary, A., Crétaux, J.-F., Frappart, F., Haines, B.

730 J., Laurain, O., Ollivier, A., Poisson, J.-C., Prandi, P., Sharma, R., Thibaut, P., and Watson, C.: The Benefits of the Ka-Band as Evidenced from the SARAL/AltiKa Altimetric Mission: Quality Assessment and Unique Characteristics of AltiKa Data, Remote Sensing, 10, 83, 2018.

Brockley, D. J.: REAPER — Product handbook for ERS Altimetry reprocessed products, 2014.

Brockley, D. J., Baker, S., Féménias, P., Martínez, B., Massmann, F., Otten, M., Paul, F., Picard, B., Prandi, P., Roca, M., Rudenko, S.,

735 Scharroo, R., and Visser, P.: REAPER: Reprocessing 12 Years of ERS-1 and ERS-2 Altimeters and Microwave Radiometer Data, IEEE Transactions on Geoscience and Remote Sensing, 55, 5506-5514, 10.1109/TGRS.2017.2709343, 2017.

Brown, G. S.: AVERAGE IMPULSE RESPONSE OF A ROUGH SURFACE AND ITS APPLICATIONS, IEEE Transactions on Antennas and Propagation, AP-25, 67-74, 1977.

Caplan, P., Derber, J., Gemmill, W., Hong, S.-Y., Pan, H.-L., and Parrish, D.: Changes to the 1995 NCEP Operational Medium-Range

740 Forecast Model Analysis–Forecast System, Weather and Forecasting, 12, 581-594, 10.1175/1520-0434(1997)012<0581:CTTNOM>2.0.CO;2, 1997.

Chelton, D. B., Walsh, E. J., and MacArthur, J. L.: Pulse Compression and Sea Level Tracking in Satellite Altimetry, Journal of Atmospheric and Oceanic Technology, 6, 407-438, 10.1175/1520-0426(1989)006<0407:PCASLT>2.0.CO;2, 1989.

Cheney, R., Lillibridge, J., and McAdoo, D.: Preliminary analysis of ERS-1 fast delivery altimeter data, Office of ocean and earth

745 sciences, NOAA National Ocean Service, Rockville, MD, 1991.

Cheney, R.: The Geosat Altimeter JGM-3 GDRs on CD-ROM, Natl. Oceanic and Atmos. Admin., Silver Spring, 1997.

Cretaux, J.-F., Nielsen, K., Frappart, F., Papa, F., Calmant, S., and Benveniste, J.: Hydrological Applications of Satellite AltimetryRivers, Lakes, Man-Made Reservoirs, Inundated Areas, in: Satellite Altimetry Over Oceans and Land Surfaces, CRC Press, 459-504, 2017.

Crétaux, J.-F., Bergé-Nguyen, M., Calmant, S., Jamangulova, N., Satylkanov, R., Lyard, F., Perosanz, F., Verron, J., Samine Montazem,

750 A., Le Guilcher, G., Leroux, D., Barrie, J., Maisongrande, P., and Bonnefond, P.: Absolute Calibration or Validation of the Altimeters on the Sentinel-3A and the Jason-3 over Lake Issykkul (Kyrgyzstan), Remote Sensing, 10, 1679, 2018.

Crétaux, J. F., Calmant, S., Romanovski, V., Shabunin, A., Lyard, F., Bergé-Nguyen, M., Cazenave, A., Hernandez, F., and Perosanz, F.: An absolute calibration site for radar altimeters in the continental domain: Lake Issykkul in Central Asia, Journal of Geodesy, 83, 723-735, 10.1007/s00190-008-0289-7, 2009.

755 Crétaux, J. F., Jelinski, W., Calmant, S., Kouraev, A., Vuglinski, V., Bergé-Nguyen, M., Gennero, M. C., Nino, F., Abarca Del Rio, R., Cazenave, A., and Maisongrande, P.: SOLS: A lake database to monitor in the Near Real Time water level and storage variations from remote sensing data, Advances in Space Research, 47, 1497-1507, 2011.

Dee, D. P., Uppala, S., Simmons, A., Berrisford, P., Poli, P., Kobayashi, S., Andrae, U., Balmaseda, M., Balsamo, G., and Bauer, d. P.: The ERA-Interim reanalysis: Configuration and performance of the data assimilation system, Quarterly Journal of the royal meteorological

760 society, 137, 553-597, 2011.

Dibarboure, G., Lamy, A., Pujol, M.-I., and Jettou, G.: The Drifting Phase of SARAL: Securing Stable Ocean Mesoscale Sampling with an Unmaintained Decaying Altitude, Remote Sensing, 10, 1051, 2018.

Donlon, C., Berruti, B., Buongiorno, A., Ferreira, M. H., Féménias, P., Frerick, J., Goryl, P., Klein, U., Laur, H., Mavrocordatos, C., Nieke, J., Rebhan, H., Seitz, B., Stroede, J., and Sciarra, R.: The Global Monitoring for Environment and Security (GMES) Sentinel-3

765 mission, Remote Sensing of Environment, 120, 37-57, 10.1016/j.rse.2011.07.024, 2012.

Duchossois, G., and Martin, P.: ERS-1 and ERS-2 tandem operations, ESA BULLETIN-EUROPEAN SPACE AGENCY, 54-60, 1995.

Fernandes, M., Lázaro, C., Nunes, A., and Scharroo, R.: Atmospheric Corrections for Altimetry Studies over Inland Water, Remote Sensing, 6, 4952, 2014.

Fernandes, M., and Lázaro, C.: GPD+ Wet Tropospheric Corrections for CryoSat-2 and GFO Altimetry Missions, Remote Sensing, 8, 851, 2016.

Frappart, F., Calmant, S., Cauhopé, M., Seyler, F., and Cazenave, A.: Preliminary results of ENVISAT RA-2-derived water levels validation over the Amazon basin, Remote Sensing of Environment, 100, 252-264, 2006.

Frappart, F., Roussel, N., Biancale, R., Martinez Benjamin, J. J., Mercier, F., Perosanz, F., Garate Pasquin, J., Martin Davila, J., Perez Gomez, B., Gracia Gomez, C., Lopez Bravo, R., Tapia Gomez, A., Gili Ripoll, J., Hernandez Pajares, M., Salazar Lino, M., Bonnefond, P., and Valles Casanova, I.: The 2013 Ibiza Calibration Campaign of Jason-2 and SARAL Altimeters, Marine Geodesy, 38, 219-232, 10.1080/01490419.2015.1008711, 2015.

Frappart, F., Legrésy, B., Niño, F., Blarel, F., Fuller, N., Fleury, S., Birol, F., and Calmant, S.: An ERS-2 altimetry reprocessing compatible with ENVISAT for long-term land and ice sheets studies, Remote Sensing of Environment, 184, 558-581, 10.1016/j.rse.2016.07.037, 2016.

Fu, L. L., Christensen, E. J., Yamarone, C. A., Lefebvre, M., Menard, Y., Dorrer, M., and Escudier, P.: TOPEX/POSEIDON mission overview, Journal of Geophysical Research: Oceans, 99, 24369-24381, 1994.

Hannah, D. M., Demuth, S., van Lanen, H. A. J., Looser, U., Prudhomme, C., Rees, G., Stahl, K., and Tallaksen, L. M.: Large-scale river flow archives: Importance, current status and future needs, Hydrological Processes, 25, 1191-1200, 10.1002/hyp.7794, 2011.

Howell, S. E. L., Brown, L. C., Kang, K.-K., and Duguay, C. R.: Variability in ice phenology on Great Bear Lake and Great Slave Lake, Northwest Territories, Canada, from SeaWinds/QuikSCAT: 2000–2006, Remote Sensing of Environment, 113, 816-834, http://dx.doi.org/10.1016/j.rse.2008.12.007, 2009.

Iijima, B. A., Harris, I. L., Ho, C. M., Lindqwister, U. J., Mannucci, A. J., Pi, X., Reyes, M. J., Sparks, L. C., and Wilson, B. D.: Automated daily process for global ionospheric total electron content maps and satellite ocean altimeter ionospheric calibration based on Global Positioning System data, Journal of Atmospheric and Solar-Terrestrial Physics, 61, 1205-1218, https://doi.org/10.1016/S1364-6826(99)00067-X, 1999.

Jarihani, A., Callow, J. N., Johansen, K., and Gouweleeuw, B.: Evaluation of multiple satellite altimetry data for studying inland water bodies and river floods, Journal of Hydrology, 505, 78-90, 10.1016/j.jhydrol.2013.09.010, 2013.

Jiang, L., Nielsen, K., Dinardo, S., Andersen, O. B., and Bauer-Gottwein, P.: Evaluation of Sentinel-3 SRAL SAR altimetry over Chinese rivers, Remote Sensing of Environment, 237, 111546, https://doi.org/10.1016/j.rse.2019.111546, 2020.

Jones, B. M., and Arp, C. D.: Observing a Catastrophic Thermokarst Lake Drainage in Northern Alaska, Permafrost and Periglacial Processes, 26, 119-128, 10.1002/ppp.1842, 2015.

Karl, T. R., Arguez, A., Huang, B., Lawrimore, J. H., McMahon, J. R., Menne, M. J., Peterson, T. C., Vose, R. S., and Zhang, H.-M.: Possible artifacts of data biases in the recent global surface warming hiatus, Science, 10.1126/science.aaa5632, 2015.

Kleinherenbrink, M., Naeije, M., Slobbe, C., Egido, A., and Smith, W.: The performance of CryoSat-2 fully-focussed SAR for inland water-level estimation, Remote Sensing of Environment, 237, 111589, https://doi.org/10.1016/j.rse.2019.111589, 2020.

Korhonen, J.: Long-term changes in lake ice cover in Finland, Hydrology Research, 37, 347-363, 2006.

Korhonen, J.: Long-term changes and variability of the winter and spring season hydrological regime in Finland, Ph.D., Institute for Atmospheric and Earth System Research University of Helsinki, Helsinki, 2019.

Lambin, J., Morrow, R., Fu, L. L., Willis, J. K., Bonekamp, H., Lillibridge, J., Perbos, J., Zaouche, G., Vaze, P., Bannoura, W., Parisot, F., Thouvenot, E., Coutin-Faye, S., Lindstrom, E., and Mignogno, M.: The OSTM/Jason-2 Mission, Marine Geodesy, 33, 4-25, 10.1080/01490419.2010.491030, 2010.

Laxon, S.: Sea ice altimeter processing scheme at the eodc, International Journal of Remote Sensing, 15, 915-924, 10.1080/01431169408954124, 1994.

Lee-Lueng, F.: TOPEX/POSEIDON mission overview, Journal of Geophysical Research, 99, 24,369-"324,381", 1994.

Lehner, B., and Döll, P.: Development and validation of a global database of lakes, reservoirs and wetlands, Journal of Hydrology, 296, 1-22, 10.1016/j.jhydrol.2004.03.028, 2004.

Lillibridge, J., Smith, W. H., Sandwell, D., Scharroo, R., Lemoine, F., and Zelensky, N.: 20 Years of Improvements to GEOSAT Altimetry, ESA Special Publication, 2006,

Liu, H., Wang, L., Tang, S. J., and Jezek, K. C.: Robust multi-scale image matching for deriving ice surface velocity field from sequential satellite images, International Journal of Remote Sensing, 33, 1799-1822, 2012.

Maillard, P., Bercher, N., and Calmant, S.: New processing approaches on the retrieval of water levels in Envisat and SARAL radar altimetry over rivers: A case study of the São Francisco River, Brazil, Remote Sensing of Environment, 156, 226-241, 10.1016/j.rse.2014.09.027, 2015.

Marsh, P., Russell, M., Pohl, S., Haywood, H., and Onclin, C.: Changes in thaw lake drainage in the Western Canadian Arctic from 1950 to 2000, Hydrological Processes, 23, 145-158, 10.1002/hyp.7179, 2009.

McConathy, D. R., and Kilgus, C. C.: The Navy GEOSAT mission: an overview, Johns Hopkins APL technical digest, 8, 170-175, 1987.

Menard, Y., Fu, L. L., Escudier, P., Parisot, F., Perbos, J., Vincent, P., Desai, S., Haines, B., and Kunstmann, G.: The Jason-1 Mission, Marine Geodesy, 26, 131-146, 10.1080/714044514, 2003.

825 Miller, M., Buizza, R., Haseler, J., Hortal, M., Janssen, P., and Untch, A.: Increased resolution in the ECMWF deterministic and ensemble prediction systems, ECMWF Newsletter, 124, 10-16, 2010.

Morris, C. S., and Gill, S. K.: Variation of Great Lakes water levels derived from Geosat altimetry, Water Resources Research, 30, 1009-1017, 10.1029/94WR00064, 1994.

MSSL/UCL/CLS: Sentinel-3 Level 2 SRAL MWR Algorithm Theoretical Baseline Definition, 138, 2019.

Normandin, C., Frappart, F., Diepkilé, A., Marieu, V., Mougin, E., Blarel, F., Lubac, B., Braquet, N., and Ba, A.: Evolution of the
830 performances of radar altimetry missions from ERS-2 to Sentinel-3A over the Inner Niger Delta, Remote Sensing, 10, 833, 2018.

Office, N. O., and Altimetry, N. L. f. S.: GeoSat Follow-On GDR User's Handbook, in, 2002.

Pavlis, N. K., Holmes, S. A., Kenyon, S. C., and Factor, J. K.: The development and evaluation of the Earth Gravitational Model 2008 (EGM2008), Journal of geophysical research: solid earth, 117, 2012.

Pekel, J.-F., Cottam, A., Gorelick, N., and Belward, A. S.: High-resolution mapping of global surface water and its long-term changes,
835 Nature, 540, 418, 10.1038/nature20584
https://www.nature.com/articles/nature20584#supplementary-information, 2016.

Pohl, S., Marsh, P., Onclin, C., and Russell, M.: The summer hydrology of a small upland tundra thaw lake: Implications to lake drainage, Hydrological Processes, 23, 2536-2546, 10.1002/hyp.7238, 2009.

Postel, S. L., Daily, G. C., and Ehrlich, P. R.: Human appropriation of renewable fresh water, Science, 271, 785-788,
840 10.1126/science.271.5250.785, 1996.

Probst, W. N., Stoll, S., Peters, L., Fischer, P., and Eckmann, R.: Lake water level increase during spring affects the breeding success of bream Abramis brama (L.), Hydrobiologia, 632, 211-224, 10.1007/s10750-009-9842-5, 2009.

Rahmstorf, S.: Thermohaline ocean circulation, Encyclopedia of quaternary sciences, 5, 2006.

Raney, R. K., and Phalippou, L.: The future of coastal altimetry, in: Coastal Altimetry, Springer, 535-560, 2011.

845 Ričko, M., Birkett, C. M., Carton, J. A., and Crétaux, J. F.: Intercomparison and validation of continental water level products derived from satellite radar altimetry, Journal of Applied Remote Sensing, 6, 2012.

Rodríguez, E., and Martin, J. M.: Assessment of the TOPEX altimeter performance using waveform retracking, Journal of Geophysical Research: Oceans, 99, 24957-24969, 10.1029/94jc02030, 1994.

Rokaya, P., Budhathoki, S., and Lindenschmidt, K. E.: Trends in the Timing and Magnitude of Ice-Jam Floods in Canada, Scientific
850 Reports, 8, 10.1038/s41598-018-24057-z, 2018.

Scharroo, R., and Smith, W. H. F.: A global positioning system–based climatology for the total electron content in the ionosphere, Journal of Geophysical Research: Space Physics, 115, 10.1029/2009ja014719, 2010.

Scharroo, R., Leuliette, E., Lillibridge, J., Byrne, D., Naeije, M., and Mitchum, G.: RADS: Consistent multi-mission products, Proc. of the Symposium on, 2013, 4,

855 Schindler, D. E., and Scheuerell, M. D.: Habitat coupling in lake ecosystems, Oikos, 98, 177-189, 10.1034/j.1600-0706.2002.980201.x, 2002.

Schwatke, C., Dettmering, D., Borgens, E., and Bosch, W.: Potential of SARAL/AltiKa for Inland Water Applications, Marine Geodesy, 38, 626-643, 10.1080/01490419.2015.1008710, 2015a.

Schwatke, C., Dettmering, D., Bosch, W., and Seitz, F.: DAHITI – an innovative approach for estimating water level time series over
860 inland waters using multi-mission satellite altimetry, Hydrol. Earth Syst. Sci., 19, 4345-4364, 10.5194/hess-19-4345-2015, 2015b.

Sentinel-3-Team: Sentinel-3 User Handbook, European Space Agency (ESA), 157, 2017.

Shu, S., Liu, H., Frappart, F., Huang, Y., Wang, S., Hinkel, K. M., Beck, R. A., Yu, B., Jones, B. M., Arp, C. D., Wang, L., and Ye, Z.: Estimation of snow accumulation over frozen Arctic lakes using repeat ICESat laser altimetry observations – A case study in northern Alaska, Remote Sensing of Environment, 216, 529-543, https://doi.org/10.1016/j.rse.2018.07.018, 2018.

865 Shu, S., Liu, H., Beck, R. A., Frappart, F., Korhonen, J., Xu, M., Yang, B., Hinkel, K. M., Huang, Y., and Yu, B.: Analysis of Sentinel-3 SAR altimetry waveform retracking algorithms for deriving temporally consistent water levels over ice-covered lakes, Remote Sensing of Environment, 239, 111643, https://doi.org/10.1016/j.rse.2020.111643, 2020.

Sulistioadi, Y. B., Tseng, K. H., Shum, C. K., Hidayat, H., Sumaryono, M., Suhardiman, A., Setiawan, F., and Sunarso, S.: Satellite radar altimetry for monitoring small rivers and lakes in Indonesia, Hydrol. Earth Syst. Sci., 19, 341-359, 10.5194/hess-19-341-2015, 2015.

870 Surdu, C. M., Duguay, C. R., Brown, L. C., and Fernández Prieto, D.: Response of ice cover on shallow lakes of the North Slope of Alaska to contemporary climate conditions (1950-2011): Radar remote-sensing and numerical modeling data analysis, Cryosphere, 8, 167-180, 2014.

Thibaut, P., Poisson, J. C., Bronner, E., and Picot, N.: Relative Performance of the MLE3 and MLE4 Retracking Algorithms on Jason-2 Altimeter Waveforms, Marine Geodesy, 33, 317-335, 10.1080/01490419.2010.491033, 2010.

875 Turner, K. W., Wolfe, B. B., Edwards, T. W. D., Lantz, T. C., Hall, R. I., and Larocque, G.: Controls on water balance of shallow thermokarst lakes and their relations with catchment characteristics: A multi-year, landscape-scale assessment based on water isotope tracers and remote sensing in Old Crow Flats, Yukon (Canada), Global Change Biology, 20, 1585-1603, 10.1111/gcb.12465, 2014.

Tyszkowski, S., Kaczmarek, H., Słowiński, M., Kozyreva, E., Brykała, D., Rybchenko, A., and Babicheva, V. A.: Geology, permafrost, and lake level changes as factors initiating landslides on Olkhon Island (Lake Baikal, Siberia), Landslides, 12, 573-583, 10.1007/s10346-880    014-0488-7, 2015.

Verpoorter, C., Kutser, T., Seekell, D. A., and Tranvik, L. J.: A global inventory of lakes based on high-resolution satellite imagery, Geophysical Research Letters, 41, 6396-6402, 10.1002/2014GL060641, 2014.

Verron, J., Sengenes, P., Lambin, J., Noubel, J., Steunou, N., Guillot, A., Picot, N., Coutin-Faye, S., Sharma, R., Gairola, R. M., Murthy, D. V. A. R., Richman, J. G., Griffin, D., Pascual, A., Rémy, F., and Gupta, P. K.: The SARAL/AltiKa Altimetry Satellite Mission, Marine 885    Geodesy, 38, 2-21, 10.1080/01490419.2014.1000471, 2015.

Villadsen, H., Deng, X., Andersen, O. B., Stenseng, L., Nielsen, K., and Knudsen, P.: Improved inland water levels from SAR altimetry using novel empirical and physical retrackers, Journal of Hydrology, 537, 234-247, 10.1016/j.jhydrol.2016.03.051, 2016.

Vu, P. L., Frappart, F., Darrozes, J., Marieu, V., Blarel, F., Ramillien, G., Bonnefond, P., and Birol, F.: Multi-Satellite Altimeter Validation along the French Atlantic Coast in the Southern Bay of Biscay from ERS-2 to SARAL, Remote Sensing, 10, 93, 2018.

Weyhenmeyer, G. A., Westöö, A. K., and Willén, E.: Increasingly ice-free winters and their effects on water quality in Sweden's largest 890    lakes, Hydrobiologia, 599, 111-118, 10.1007/s10750-007-9188-9, 2008.

Williamson, C. E., Saros, J. E., Vincent, W. F., and Smol, J. P.: Lakes and reservoirs as sentinels, integrators, and regulators of climate change, Limnology and Oceanography, 54, 2273-2282, 2009.

Wingham, D. J., Rapley, C. G., and Griffiths, H.: NEW TECHNIQUES IN SATELLITE ALTIMETER TRACKING SYSTEMS, Digest - 895    International Geoscience and Remote Sensing Symposium (IGARSS), 1986, 1339-1344,

Wingham, D. J., Francis, C. R., Baker, S., Bouzinac, C., Brockley, D., Cullen, R., de Chateau-Thierry, P., Laxon, S. W., Mallow, U., Mavrocordatos, C., Phalippou, L., Ratier, G., Rey, L., Rostan, F., Viau, P., and Wallis, D. W.: CryoSat: A mission to determine the fluctuations in Earth's land and marine ice fields, Advances in Space Research, 37, 841-871, 2006.

Zandbergen, R., Dow, J. M., Romay Merino, M., Píriz, R., and Martínez Fadrique, F.: ERS-1 and ERS-2 tandem mission: Orbit 900    determination, prediction and maintenance, Advances in Space Research, 19, 1649-1653, https://doi.org/10.1016/S0273-1177(97)00319-0, 1997.

Zelli, C.: ENVISAT RA-2 advanced radar altimeter: instrument design and pre-launch performance assessment review, Acta Astronautica, 44, 323-333, 10.1016/S0094-5765(99)00063-6, 1999.

Ziyad, J., Goïta, K., Magagi, R., Blarel, F., and Frappart, F.: Improving the Estimation of Water Level over Freshwater Ice Cover using 905    Altimetry Satellite Active and Passive Observations, Remote Sensing, 12, 967, 2020.

**Table 1.** Geographical characteristics of case study lakes and gauge stations

| | | | | | | | Gauge Stations | |
|---|---|---|---|---|---|---|---|---|
| **Lakes** | | | | | | | **Gauge Stations** | |
| Index | Name | Country | Lat(°) | Lon(°) | Area (km$^2$) | Winter ice cover | Name | Datum |
| 1 | Inarijarvi | | 69.02 | 27.89 | 1184 | Fully | Nellim | N2000 |
| 2 | Lokka | Finland | 67.96 | 27.63 | 487 | Fully | Lokka | N2000 |
| 3 | Oulujarvi | | 64.35 | 27.21 | 889 | Fully | Vuottolahti | N2000 |
| 4 | Vanern | Sweden | 58.91 | 13.30 | 5550 | None or Partly | Vanern | RH00 |
| 5 | Great Slave | | 61.80 | -113.82 | 27816 | Fully | YellowKnife | CGVD28 |
| 6 | Athabasca | Canada | 59.18 | -109.34 | 7781 | Fully | CrackingStone | CGVD28 |
| 7 | Cedar | | 53.34 | -100.16 | 2817 | Fully | Oleson Point | CGVD28 |
| 8 | Superior | | 47.54 | -87.76 | 81935 | Fully or Partly | Ontonagon | IGLD85 |
| 9 | Huron | US & | 44.96 | -82.26 | 59756 | Partly | Lakeport | IGLD85 |
| 10 | Ontario | Canada | 43.67 | -77.76 | 19328 | Partly | Rochester | IGLD85 |
| 11 | Erie | | 42.16 | -81.24 | 25691 | Fully or Partly | Cleveland | IGLD85 |
| 12 | Michigan | US | 44.01 | -86.76 | 57399 | Partly | Calumet Harbor | IGLD85 |

* The areas and geographic coordinates are derived from GLWD

**Table 2.** The eleven satellite radar altimetry missions and their data products

| Mission | Operational Time Begin | Operational Time End | Organization | Geographic Coverage | Repeat Cycle | Data Product Source | Data Product Rate | Data Product Retrackers | MWR Bands (GHz) |
|---|---|---|---|---|---|---|---|---|---|
| GeoSat | 03/12/1985 | 01/01/1990 | U.S. Navy | 72°N–72°S | 17 days | RADS | 1 Hz | Ocean | — |
| ERS-1 | 07/17/1991 | 03/10/2000 | ESA | 81.5°N–81.5°S | 35 days | ESA | 20 Hz | Ice1, Ice2, Ocean, Sea-Ice | 23.8, 36.5 |
| T/P | 08/10/1992 | 10/09/2005 | NASA, CNES | 66°N–66°S | 10 days | RADS | 1 Hz | Ocean | 18, 21, 37 |
| ERS-2 | 04/21/1995 | 09/05/2011 | ESA | 81.5°N–81.5°S | 35 days | CTOH | 20 Hz | Ice1, Ice2 | 23.8, 36.5 |
| GFO | 02/10/1998 | 10/22/2008 | U.S. Navy | 72°N–72°S | 17 days | NOAA | 10 Hz | Ocean | 22, 37 |
| Jason-1 | 12/07/2001 | 07/01/2013 | NASA, CNES | 66°N–66°S | 10 days | AVISO+ | 20 Hz | MLE4, Ice | 18.7, 23.8, 34 |
| ~~ENVISat~~ENVISAT | 02/28/2002 | 04/08/2012 | ESA | 81.5°N–81.5°S | 35 days | ESA | 18 Hz | Ice1, Ice2, Ocean, Sea-Ice | 23.8, 36.5 |
| Jason-2 | 06/20/2008 | 10/01/2019 | NASA, CNES, NOAA, EUMETSAT | 66°N–66°S | 10 days | AVISO+ | 20 Hz | MLE4, Ice | 18.7, 23.8, 34 |
| SARAL | 02/25/2013 | — | CNES, ISRO | 81.5°N–81.5°S | 35 days | AVISO+ | 40 Hz | Ice1, Ice2, Ocean, Sea-Ice | 23.8, 37 |
| Jason-3 | 01/17/2016 | — | NASA, CNES, NOAA, EUMETSAT | 66°N–66°S | 10 days | AVISO+ | 20 Hz | MLE4, Ice | 18.7, 23.8, 34 |
| Sentinel-3A Sentinel-3B | 02/16/2016 04/25/2018 | — | ESA | 81.35°N–81.35°S | 27 days | ESA | 20 Hz | OCOG, Ice-Sheet, Sea-Ice, SAMOSA-2~~3~~ | 23.8, 36.5 |

910

**Table 3.** The version of altimetry data product, the models of the three atmospheric corrections.

| Mission | Data Source | Version | Ionospheric Correction ($\Delta R_{iono}$) | Wet Tropospheric Correction ($\Delta R_{wet}$) | Dry Tropospheric Correction ($\Delta R_{dry}$) |
|---|---|---|---|---|---|
| GeoSat | RADS | — | NIC09 | ERA | ERA |
| ERS-1 | ESA | REAPER | NIC09 | ERA | ERA |
| T/P | RADS | GDR-M | NIC09, GIM | ERA | ERA |
| ERS-2 | CTOH | CTOH | NIC09, GIM | ERA | ERA |
| GFO | NOAA | GDR | GIM | NCEP | NCEP |
| Jason-1 | AVISO+ | GDR-E | GIM | ERA | ERA |
| ~~ENVISat~~ENVISAT | ESA | V3 | GIM | ECMWF | ECMWF |
| Jason-2 | AVISO+ | GDR-D | GIM | ECMWF | ECMWF |
| SARAL | AVISO+ | GDR-T | GIM | ECMWF | ECMWF |
| Jason-3 | AVISO+ | GDR-D | GIM | ECMWF | ECMWF |
| Sentinel-3 | ESA | Baseline-2.45 | GIM | ECMWF | ECMWF |

**Table 4.** The indices of ground tracks selected for each satellite mission over each lake

| Mission Name | Phase | Cycles | Inarijarvi | Lokka | Oulujarvi | Vanern | GreatSlave | Athabasca | Cedar | Superior | Huron | Ontario | Erie | Michigan |
|---|---|---|---|---|---|---|---|---|---|---|---|---|---|---|
| GeoSat | Nominal | 67 | 367 | 104 | 397 | 399 | 28 | 228 | 198 | 168 | 293 | 52 | 368 | 24 |
| ERS-1 | Nominal | 32 | 197 | 283 | 541 | 846 | 570 | 409 | 912 | 93 | 80 | 493 | 751 | 93 |
| T/P | Nominal | 333 | — | — | 239 | 144 | 223 | 95 | 178 | 254 | 117 | 15 | 193 | 41 |
| | Intermittent | 111 | — | — | 116 | 220 | 45 | 171 | 195 | 76 | 152 | 50 | 152 | 254 |
| ERS-2 | Nominal | 90 | 197 | 283 | 541 | 846 | 570 | 409 | 912 | 93 | 80 | 493 | 751 | 93 |
| GFO | Nominal | 180 | 367 | 104 | 397 | 399 | 28 | 228 | 198 | 168 | 293 | 52 | 368 | 24 |
| Jason-1 | Nominal | 259 | — | — | 239 | 144 | 223 | 95 | 178 | 254 | 117 | 15 | 193 | 41 |
| | Intermittent | 113 | — | — | 116 | 220 | 45 | 171 | 195 | 76 | 152 | 50 | 152 | 254 |
| ENVISatE NVISAT | Nominal | 89 | 197 | 283 | 541 | 846 | 570 | 409 | 912 | 93 | 80 | 493 | 751 | 93 |
| | Extension | 19 | 169 | 399 | 543 | 648 | 802 | 37 | 312 | 512 | 224 | 581 | 409 | 52 |
| Jason-2 | Nominal | 304 | — | — | 239 | 144 | 223 | 95 | 178 | 254 | 117 | 15 | 193 | 41 |
| | Intermittent | 23 | — | — | 116 | 220 | 45 | 171 | 195 | 76 | 152 | 50 | 152 | 254 |
| SARAL | Nominal | 34 | 197 | 283 | 541 | 846 | 570 | 409 | 912 | 93 | 80 | 493 | 751 | 93 |
| Jason-3 | Nominal | 78 | — | — | 239 | 144 | 223 | 95 | 178 | 254 | 117 | 15 | 193 | 41 |
| Sentinel-3 | Nominal | 18 | 272 | 386 | 72 | 358 | 682 | 54 | 766 | 549 | 422 | 222 | 650 | 736 |

Note that there are no T/P and Jason overpasses for Lake Inarijarvi and Lokka, since their geographic coverage is up to latitude of 66°N.

**Table 5.** The number of lake water level estimates during ice-free (open water) and ice-covered seasons

| Mission | | | Inarijarvi | | Lokka | | Oulujarvi | | Vanern | | GreatSlave | | Athabasca | | Cedar | | Superior | | Huron | | Ontario | | Erie | | Michigan | |
|---|---|---|---|---|---|---|---|---|---|---|---|---|---|---|---|---|---|---|---|---|---|---|---|---|---|---|---|
| Name | Cycles | Retracker | ice | water | ice | water | ice | water | ice | water | ice | water | ice | water | ice | water | ice | water | ice | water | ice | water | ice | water | ice | water |
| GeoSat | 67 | Ocean | 16 | 1 | 6 | 1 | 9 | 2 | 5 | 7 | 9 | 10 | 11 | 7 | 0 | 1 | 10 | 28 | 3 | 31 | 0 | 29 | 8 | 41 | 9 | 34 |
| ERS-1 | 32 | Ice1 | 11 | 10 | 14 | 8 | 14 | 11 | 3 | 26 | 14 | 9 | 11 | 13 | 14 | 14 | 5 | 25 | 7 | 18 | 4 | 26 | 4 | 24 | 6 | 26 |
| ERS-1 | | Ice2 | 11 | 9 | 14 | 8 | 14 | 11 | 3 | 26 | 14 | 9 | 11 | 13 | 14 | 14 | 5 | 24 | 7 | 19 | 4 | 26 | 4 | 24 | 6 | 26 |
| ERS-1 | | Sea-Ice | 11 | 10 | 14 | 8 | 14 | 13 | 3 | 26 | 14 | 9 | 11 | 13 | 14 | 14 | 5 | 24 | 7 | 18 | 4 | 22 | 4 | 23 | 6 | 23 |
| ERS-1 | | Ocean | 7 | 7 | 10 | 7 | 10 | 12 | 3 | 26 | 11 | 9 | 7 | 13 | 9 | 12 | 2 | 23 | 4 | 17 | 3 | 22 | 1 | 23 | 4 | 23 |
| T/P | 444 | Ocean | | | | | 234 | 166 | 15 | 140 | 191 | 122 | 181 | 217 | 183 | 187 | 35 | 300 | 37 | 325 | 43 | 364 | 61 | 313 | 63 | 361 |
| ERS-2 | 90 | Ice1 | 38 | 28 | 30 | 39 | 31 | 21 | 6 | 59 | 35 | 32 | 27 | 34 | 28 | 34 | 12 | 56 | 14 | 64 | 12 | 70 | 12 | 57 | 14 | 53 |
| ERS-2 | | Ice2 | 38 | 33 | 30 | 39 | 31 | 21 | 6 | 59 | 35 | 32 | 27 | 34 | 28 | 34 | 12 | 56 | 14 | 64 | 12 | 70 | 12 | 57 | 14 | 53 |
| GFO | 180 | Ocean | 41 | 7 | 92 | 14 | 46 | 7 | 15 | 96 | 70 | 36 | 56 | 42 | 28 | 8 | 9 | 134 | 16 | 107 | 19 | 125 | 21 | 112 | 34 | 125 |
| Jason-1 | 372 | Ice | — | — | — | — | 160 | 149 | 67 | 134 | 206 | 133 | 185 | 193 | 171 | 165 | 42 | 301 | 55 | 293 | 58 | 291 | 31 | 297 | 70 | 279 |
| Jason-1 | | MLE4 | — | — | — | — | 88 | 121 | 24 | 90 | 180 | 127 | 176 | 170 | 155 | 118 | 36 | 300 | 48 | 291 | 58 | 291 | 19 | 302 | 70 | 279 |
| ENVISAT | 108 | Ice1 | 48 | 45 | 38 | 50 | 38 | 51 | 13 | 85 | 36 | 44 | 45 | 45 | 44 | 45 | 7 | 78 | 11 | 78 | 17 | 84 | 12 | 72 | 15 | 84 |
| ENVISAT | | Ice2 | 48 | 43 | 38 | 50 | 38 | 52 | 13 | 85 | 36 | 44 | 45 | 45 | 44 | 45 | 7 | 79 | 11 | 78 | 17 | 84 | 12 | 72 | 14 | 84 |
| ENVISAT | | Sea-Ice | 48 | 42 | 38 | 49 | 38 | 41 | 13 | 84 | 36 | 44 | 45 | 45 | 44 | 45 | 7 | 79 | 11 | 78 | 17 | 84 | 12 | 72 | 15 | 84 |
| ENVISAT | | Ocean | 48 | 45 | 38 | 50 | 38 | 48 | 13 | 85 | 36 | 44 | 45 | 45 | 44 | 45 | 7 | 75 | 11 | 78 | 17 | 84 | 12 | 72 | 15 | 84 |
| Jason-2 | 327 | Ice | — | — | — | — | 153 | 125 | 54 | 172 | 189 | 128 | 178 | 179 | 172 | 152 | 32 | 282 | 34 | 284 | 58 | 258 | 50 | 272 | 48 | 273 |
| Jason-2 | | MLE4 | — | — | — | — | 83 | 102 | 21 | 95 | 161 | 120 | 168 | 162 | 141 | 143 | 28 | 281 | 33 | 283 | 58 | 251 | 37 | 272 | 47 | 273 |
| SARAL | 35 | Ice1 | 16 | 18 | 18 | 16 | 16 | 18 | 1 | 33 | 18 | 16 | 13 | 16 | 16 | 18 | 4 | 29 | 6 | 29 | 6 | 29 | 5 | 29 | 6 | 16 |
| SARAL | | Ice2 | 16 | 16 | 18 | 16 | 16 | 16 | 1 | 33 | 18 | 16 | 13 | 16 | 16 | 18 | 4 | 30 | 6 | 29 | 6 | 29 | 5 | 29 | 6 | 16 |
| SARAL | | Sea-Ice | 16 | 17 | 18 | 16 | 16 | 14 | 1 | 33 | 18 | 16 | 13 | 16 | 16 | 18 | 4 | 30 | 6 | 29 | 6 | 29 | 5 | 29 | 6 | 16 |
| SARAL | | Ocean | 16 | 17 | 18 | 16 | 16 | 15 | 1 | 33 | 18 | 16 | 13 | 16 | 16 | 18 | 4 | 30 | 6 | 29 | 6 | 29 | 5 | 29 | 6 | 16 |
| Jason-3 | 79 | Ice | — | — | — | — | 42 | 27 | 7 | 62 | 43 | 28 | 43 | 35 | 41 | 38 | 8 | 66 | 3 | 72 | 6 | 67 | 8 | 70 | 6 | 69 |
| Jason-3 | | MLE4 | — | — | — | — | 23 | 28 | 3 | 36 | 38 | 25 | 37 | 35 | 35 | 35 | 7 | 66 | 3 | 72 | 6 | 66 | 6 | 70 | 6 | 69 |
| Sentinel-3 | 18 | Ice-Sheet | 7 | 10 | 7 | 11 | 7 | 9 | 0 | 18 | 7 | 11 | 7 | 11 | 6 | 10 | 0 | 18 | 0 | 18 | 0 | 18 | 0 | 18 | 0 | 18 |
| Sentinel-3 | | OCOG | 7 | 10 | 7 | 11 | 7 | 9 | 0 | 18 | 7 | 11 | 7 | 11 | 6 | 10 | 0 | 18 | 0 | 18 | 0 | 18 | 0 | 18 | 0 | 18 |
| Sentinel-3 | | SAMOSA2 | 7 | 10 | 7 | 11 | 7 | 9 | 0 | 18 | 7 | 11 | 7 | 11 | 6 | 10 | 0 | 18 | 0 | 18 | 0 | 18 | 0 | 18 | 0 | 18 |

915

**Table 6.** The data loss rate for lake water level estimates over each lake for each retracker

| Mission | | | Rate of Missing Estimates (%) | | | | | | | | | | | | Mean |
|---|---|---|---|---|---|---|---|---|---|---|---|---|---|---|---|
| Name | Cycles | Retracker | Inarijarvi | Lokka | Oulujarvi | Vanern | GreatSlave | Athabasca | Cedar | Superior | Huron | Ontario | Erie | Michigan | |
| GeoSat | 57 | Ocean | 74.63 | 89.55 | 83.58 | 82.09 | 71.64 | 73.13 | 98.51 | 43.28 | 49.25 | 56.72 | 26.87 | 35.82 | 65.42 |
| ERS-1 | 32 | Ice1 | 34.38 | 31.25 | 21.88 | 9.38 | 28.13 | 25.00 | 12.50 | 6.25 | 21.88 | 6.25 | 12.50 | 0.00 | 17.45 |
| | | Ice2 | 37.50 | 31.25 | 21.88 | 9.38 | 28.13 | 25.00 | 12.50 | 9.38 | 18.75 | 6.25 | 12.50 | 0.00 | 17.71 |
| | | Sea-Ice | 34.38 | 31.25 | 15.63 | 9.38 | 28.13 | 25.00 | 12.50 | 9.38 | 21.88 | 18.75 | 15.63 | 9.38 | 19.27 |
| | | Ocean | 56.25 | 46.88 | 31.25 | 9.38 | 37.50 | 37.50 | 34.38 | 21.88 | 34.38 | 21.88 | 25.00 | 15.63 | 30.99 |
| T/P | 444 | Ocean | — | — | 9.91 | 65.09 | 29.50 | 10.36 | 16.67 | 24.55 | 18.47 | 8.33 | 15.77 | 4.50 | 20.32 |
| ERS-2 | 90 | Ice1 | 26.67 | 23.33 | 42.22 | 27.78 | 25.56 | 32.22 | 31.11 | 24.44 | 13.33 | 8.89 | 23.33 | 25.56 | 25.37 |
| | | Ice2 | 21.11 | 23.33 | 42.22 | 27.78 | 25.56 | 32.22 | 31.11 | 24.44 | 13.33 | 8.89 | 23.33 | 25.56 | 24.91 |
| GFO | 180 | Ocean | 73.33 | 41.11 | 70.56 | 38.33 | 41.11 | 45.56 | 80.00 | 20.56 | 31.67 | 20.00 | 26.11 | 11.67 | 41.67 |
| Jason-1 | 372 | Ice | — | — | 16.94 | 45.97 | 8.87 | 8.06 | 9.68 | 7.80 | 6.45 | 6.18 | 11.83 | 6.18 | 12.80 |
| | | MLE4 | — | — | 43.82 | 69.35 | 17.47 | 12.90 | 26.61 | 9.68 | 8.87 | 6.18 | 13.71 | 6.18 | 21.48 |
| ~~ENVISatE~~ NVISAT | 108 | Ice1 | 13.89 | 18.52 | 17.59 | 9.26 | 25.93 | 16.67 | 17.59 | 21.30 | 17.59 | 6.48 | 22.22 | 8.33 | 16.28 |
| | | Ice2 | 15.74 | 18.52 | 16.67 | 9.26 | 25.93 | 16.67 | 17.59 | 20.37 | 17.59 | 6.48 | 22.22 | 9.26 | 16.36 |
| | | Sea-Ice | 16.67 | 19.44 | 26.85 | 10.19 | 25.93 | 16.67 | 17.59 | 20.37 | 17.59 | 6.48 | 22.22 | 8.33 | 17.36 |
| | | Ocean | 13.89 | 18.52 | 20.37 | 9.26 | 25.93 | 16.67 | 17.59 | 24.07 | 17.59 | 6.48 | 22.22 | 8.33 | 16.74 |
| Jason-2 | 327 | Ice | — | — | 14.98 | 30.89 | 3.06 | 2.75 | 0.92 | 3.98 | 2.75 | 3.36 | 1.53 | 1.83 | 6.61 |
| | | MLE4 | — | — | 43.43 | 64.53 | 14.07 | 7.34 | 13.15 | 5.50 | 3.36 | 5.50 | 5.50 | 2.14 | 16.45 |
| SARAL | 35 | Ice1 | 2.86 | 2.86 | 2.86 | 2.86 | 2.86 | 17.14 | 2.86 | 5.71 | 0.00 | 0.00 | 2.86 | 37.14 | 6.67 |
| | | Ice2 | 8.57 | 2.86 | 8.57 | 2.86 | 2.86 | 17.14 | 2.86 | 2.86 | 0.00 | 0.00 | 2.86 | 37.14 | 7.38 |
| | | Sea-Ice | 5.71 | 2.86 | 14.29 | 2.86 | 2.86 | 17.14 | 2.86 | 2.86 | 0.00 | 0.00 | 2.86 | 37.14 | 7.62 |
| | | Ocean | 5.71 | 2.86 | 11.43 | 2.86 | 2.86 | 17.14 | 2.86 | 2.86 | 0.00 | 0.00 | 2.86 | 37.14 | 7.38 |
| Jason-3 | 79 | Ice | — | — | 12.66 | 12.66 | 10.13 | 1.27 | 0.00 | 6.33 | 5.06 | 7.59 | 1.27 | 5.06 | 6.20 |
| | | MLE4 | — | — | 35.44 | 50.63 | 20.25 | 8.86 | 11.39 | 7.59 | 5.06 | 8.86 | 3.80 | 5.06 | 15.70 |
| Sentinel-3 | 18 | Ice-Sheet | 5.56 | 0.00 | 11.11 | 0.00 | 0.00 | 0.00 | 11.11 | 0.00 | 0.00 | 0.00 | 0.00 | 0.00 | 2.32 |
| | | OCOG | 5.56 | 0.00 | 11.11 | 0.00 | 0.00 | 0.00 | 11.11 | 0.00 | 0.00 | 0.00 | 0.00 | 0.00 | 2.32 |
| | | SAMOSA~3~ 2 | 5.56 | 0.00 | 11.11 | 0.00 | 0.00 | 0.00 | 11.11 | 0.00 | 0.00 | 0.00 | 0.00 | 0.00 | 2.32 |

920

**Table 7.** The *Bias* between altimetry-derived estimates and gauge measurements

| Mission | | *Bias* (cm) | | | | | | | | | | | | Mean* | STD* |
|---------|-----------|------------|-------|----------|--------|-----------|-----------|--------|----------|--------|---------|--------|----------|-------|------|
| Name | Retracker | Inarijarvi | Lokka | Oulujarvi | Vanern | GreatSlave | Athabasca | Cedar | Superior | Huron | Ontario | Erie | Michigan | | |
| GeoSat | Ocean | — | — | — | 34.77 | 45.28 | -1.41 | — | 25.10 | 42.36 | 45.59 | 87.61 | 54.20 | 50.97 | 23.05 |
| ERS-1 | Ice1 | 39.23 | 26.05 | 17.43 | 89.40 | 85.69 | 47.43 | 76.69 | 64.18 | 93.36 | 80.85 | 88.40 | 82.14 | 81.79 | 11.05 |
| | Ice2 | 41.60 | 38.26 | 1.18 | 73.43 | 76.48 | 44.64 | 67.18 | 52.13 | 81.08 | 70.66 | 75.67 | 73.48 | 70.60 | 11.01 |
| | Sea-Ice | 38.39 | 17.45 | -20.52 | 62.75 | 76.74 | 43.62 | 64.79 | 53.44 | 77.73 | 69.18 | 73.46 | 71.32 | 69.03 | 9.27 |
| | Ocean | -41.99 | 67.73 | -14.59 | 66.18 | 87.11 | 34.50 | 46.86 | 47.12 | 77.07 | 65.54 | 69.51 | 65.57 | 64.96 | 11.03 |
| T/P | Ocean | — | — | -116.44 | -27.77 | -5.46 | -19.43 | -28.56 | -16.63 | -1.35 | -0.86 | 10.25 | 14.68 | 1.22 | 12.17 |
| ERS-2 | Ice1 | 87.95 | 59.19 | 19.68 | 85.99 | 96.83 | 71.89 | 96.21 | 78.54 | 95.75 | 96.23 | 100.36 | 96.80 | 93.54 | 8.58 |
| | Ice2 | 77.60 | 35.71 | -20.72 | 49.60 | 61.36 | 35.22 | 64.79 | 39.56 | 59.15 | 56.23 | 59.19 | 55.82 | 53.99 | 8.22 |
| GFO | Ocean | -30.49 | -8.05 | -106.08 | 36.98 | 81.16 | 68.83 | 49.58 | 68.81 | 79.90 | 83.97 | 90.97 | 84.35 | 81.60 | 8.18 |
| Jason-1 | Ice | — | — | -47.86 | 18.58 | 23.21 | 11.32 | 20.00 | 10.51 | 26.95 | 26.76 | 35.91 | 39.76 | 27.98 | 11.28 |
| | MLE4 | — | — | -154.03 | 4.36 | 2.44 | -7.85 | -11.17 | -13.08 | 2.45 | 3.68 | 11.88 | 15.44 | 4.07 | 11.04 |
| ~~ENVISatE~~ NVISAT | Ice1 | 25.24 | 18.92 | 11.10 | 75.56 | 73.60 | 49.62 | 59.12 | 59.45 | 74.86 | 77.02 | 79.09 | 74.46 | 72.98 | 7.79 |
| | Ice2 | -3.01 | -0.94 | -17.77 | 51.27 | 48.68 | 25.60 | 39.09 | 34.06 | 47.95 | 49.40 | 52.53 | 47.54 | 46.30 | 7.12 |
| | Sea-Ice | -13.30 | -19.44 | -47.46 | 44.66 | 43.22 | 19.14 | 31.80 | 28.44 | 42.29 | 43.00 | 47.20 | 41.25 | 40.44 | 7.08 |
| | Ocean | 23.45 | 26.75 | -13.65 | 49.78 | 48.22 | 25.43 | 44.58 | 32.31 | 48.48 | 47.87 | 52.17 | 46.52 | 45.47 | 7.65 |
| Jason-2 | Ice | — | — | -28.43 | 36.37 | 44.96 | 36.08 | 18.60 | 19.81 | 48.37 | 49.24 | 57.12 | 60.64 | 47.04 | 16.08 |
| | MLE4 | — | — | -165.82 | -31.22 | 5.68 | -4.12 | -13.54 | -14.50 | 1.29 | 4.33 | 11.34 | 14.55 | 3.40 | 11.33 |
| SARAL | Ice1 | 38.85 | 28.92 | 33.60 | 84.11 | 79.71 | 79.46 | 58.24 | 81.61 | 77.72 | 97.40 | 101.24 | 94.69 | 90.53 | 10.28 |
| | Ice2 | 25.77 | 26.31 | 22.50 | 70.74 | 67.02 | 65.49 | 49.05 | 67.39 | 62.30 | 84.32 | 85.00 | 79.91 | 75.78 | 10.33 |
| | Sea-Ice | 11.05 | 3.08 | -7.18 | 64.07 | 60.73 | 58.56 | 40.20 | 60.23 | 54.30 | 77.74 | 77.48 | 72.82 | 68.51 | 10.66 |
| | Ocean | 21.30 | -5.71 | -13.91 | 75.36 | 71.05 | 50.69 | 49.22 | 51.57 | 66.04 | 69.78 | 69.24 | 64.81 | 64.29 | 7.41 |
| Jason-3 | Ice | — | — | -46.73 | 11.14 | 23.82 | 20.14 | 0.81 | -0.82 | 26.32 | 29.03 | 36.35 | 39.99 | 26.17 | 16.06 |
| | MLE4 | — | — | -189.09 | 0.98 | 6.78 | -2.91 | -12.36 | -16.63 | -1.70 | 2.28 | 7.19 | 11.26 | 0.48 | 10.75 |
| Sentinel-3 | Ice-Sheet | -36.19 | -19.60 | -33.72 | 21.27 | 19.64 | -0.40 | 13.57 | 1.52 | 11.96 | 3.16 | 17.90 | 9.50 | 8.81 | 6.67 |
| | OCOG | -25.99 | -34.81 | -16.17 | 45.17 | 42.47 | 23.08 | -2.90 | 26.72 | 37.95 | 28.60 | 42.93 | 35.22 | 34.28 | 6.68 |
| | SAMOSA~~2~~2̲3̶ | -37.01 | -19.33 | -42.15 | 14.18 | 12.95 | -7.00 | 4.08 | -6.35 | 4.86 | -3.96 | 10.94 | 2.26 | 1.55 | 6.94 |

* The mean *Bias* and the standard deviation (STD) were computed for each retracker using only the *Biases* on the Great Lakes.

**Table 8.** The Pearson's correlation coefficient *r* between altimetry-derived lake level estimates and *gauge* measurements

| Mission Name | Retracker | Inarijarvi | Lokka | Oulujarvi | Vanern | GreatSlave | Athabasca | Cedar | Superior | Huron | Ontario | Erie | Michigan | Mean |
|---|---|---|---|---|---|---|---|---|---|---|---|---|---|---|
| GeoSat | Ocean | — | — | — | 0.45 | 0.13 | 0.84 | — | 0.78 | 0.94 | 0.93 | 0.88 | 0.93 | 0.74 |
| ERS-1 | Ice1 | 0.56 | 0.79 | 0.80 | 0.97 | 0.98 | 0.94 | 0.94 | 0.76 | 0.94 | 0.97 | 0.91 | 0.76 | 0.86 |
| | Ice2 | 0.29 | 0.62 | 0.65 | 0.84 | 0.73 | 0.93 | 0.66 | 0.69 | 0.61 | 0.94 | 0.88 | 0.80 | 0.72 |
| | Sea-Ice | 0.35 | 0.66 | 0.49 | 0.63 | 0.41 | 0.75 | 0.70 | 0.10 | 0.35 | 0.71 | 0.43 | 0.47 | 0.50 |
| | Ocean | 0.70 | 0.68 | 0.07 | 0.90 | 0.73 | 0.94 | 0.38 | 0.83 | 0.72 | 0.97 | 0.92 | 0.87 | 0.73 |
| T/P | Ocean | — | — | 0.21 | 0.58 | 0.84 | 0.97 | 0.93 | 0.97 | 0.99 | 0.98 | 0.98 | 0.99 | 0.84 |
| ERS-2 | Ice1 | 0.62 | 0.89 | 0.57 | 0.95 | 0.93 | 0.99 | 0.96 | 0.79 | 0.96 | 0.91 | 0.96 | 0.96 | 0.87 |
| | Ice2 | 0.24 | 0.76 | 0.41 | 0.94 | 0.87 | 0.99 | 0.90 | 0.75 | 0.95 | 0.86 | 0.93 | 0.95 | 0.80 |
| GFO | Ocean | 0.95 | 0.47 | 0.14 | 0.95 | 0.91 | 0.97 | 0.80 | 0.92 | 0.93 | 0.98 | 0.95 | 0.92 | 0.82 |
| Jason-1 | Ice | — | — | 0.77 | 0.89 | 0.94 | 0.98 | 0.91 | 0.96 | 0.94 | 0.99 | 0.95 | 0.93 | 0.93 |
| | MLE4 | — | — | 0.22 | 0.89 | 0.94 | 0.99 | 0.93 | 0.96 | 0.95 | 0.99 | 0.96 | 0.93 | 0.88 |
| ~~ENVISatE~~ NVISAT | Ice1 | 0.82 | 0.99 | 0.94 | 0.99 | 0.96 | 0.99 | 0.98 | 0.97 | 0.94 | 0.97 | 0.97 | 0.88 | 0.95 |
| | Ice2 | 0.72 | 0.98 | 0.78 | 0.99 | 0.96 | 0.99 | 0.97 | 0.97 | 0.96 | 0.98 | 0.98 | 0.94 | 0.94 |
| | Sea-Ice | 0.46 | 0.97 | 0.69 | 0.98 | 0.92 | 0.98 | 0.95 | 0.96 | 0.95 | 0.97 | 0.98 | 0.93 | 0.90 |
| | Ocean | 0.46 | 0.91 | 0.68 | 0.97 | 0.86 | 0.98 | 0.85 | 0.98 | 0.90 | 0.97 | 0.98 | 0.93 | 0.87 |
| Jason-2 | Ice | — | — | 0.75 | 0.85 | 0.92 | 0.99 | 0.94 | 0.98 | 0.97 | 0.98 | 0.96 | 0.97 | 0.93 |
| | MLE4 | — | — | 0.29 | 0.18 | 0.95 | 0.99 | 0.88 | 0.98 | 0.98 | 0.99 | 0.98 | 0.98 | 0.82 |
| SARAL | Ice1 | 0.87 | 0.93 | 0.93 | 0.98 | 0.97 | 0.99 | 0.89 | 0.97 | 0.96 | 0.99 | 0.94 | 0.98 | 0.95 |
| | Ice2 | 0.85 | 0.92 | 0.87 | 0.99 | 0.99 | 0.99 | 0.72 | 0.98 | 0.98 | 0.99 | 0.99 | 0.99 | 0.94 |
| | Sea-Ice | 0.85 | 0.89 | 0.67 | 0.99 | 0.99 | 0.99 | 0.81 | 0.99 | 0.99 | 0.99 | 0.99 | 0.99 | 0.93 |
| | Ocean | 0.75 | 0.90 | 0.56 | 0.99 | 0.99 | 0.99 | 0.79 | 0.98 | 0.97 | 0.99 | 0.98 | 0.99 | 0.91 |
| Jason-3 | Ice | — | — | 0.52 | 0.66 | 0.93 | 0.99 | 0.95 | 0.97 | 0.95 | 0.99 | 0.97 | 0.95 | 0.89 |
| | MLE4 | — | — | 0.53 | 0.24 | 0.94 | 0.99 | 0.93 | 0.95 | 0.95 | 0.99 | 0.96 | 0.93 | 0.84 |
| Sentinel-3 | Ice-Sheet | 0.98 | 0.86 | 0.74 | 0.98 | 0.97 | 0.99 | 0.81 | 0.95 | 0.98 | 0.99 | 0.99 | 0.96 | 0.93 |
| | OCOG | 0.99 | 0.90 | 0.98 | 0.98 | 0.97 | 0.99 | 0.86 | 0.97 | 0.98 | 0.99 | 0.98 | 0.95 | 0.96 |
| | SAMOSA~~2~~3 | 0.99 | 0.89 | 0.90 | 0.99 | 0.97 | 0.99 | 0.78 | 0.91 | 0.98 | 0.99 | 0.99 | | 0.96 | 0.94 |

925

**Table 9.** The *RMSE* between altimetry-derived lake water level estimates and gauge measurements

| Mission | | *RMSE* (cm) | | | | | | | | | | | | Mean | STD |
|---|---|---|---|---|---|---|---|---|---|---|---|---|---|---|---|
| Name | Retracker | Inarijarvi | Lokka | Oulujarvi | Vanern | GreatSlave | Athabasca | Cedar | Superior | Huron | Ontario | Erie | Michigan | | |
| GeoSat | Ocean | — | — | — | 23.74 | 45.28 | 10.00 | — | 8.80 | 9.19 | 9.03 | 13.08 | 10.09 | 16.15 | 11.95 |
| ERS-1 | Ice1 | 53.16 | 33.01 | 17.91 | 4.75 | 5.49 | 9.16 | 9.72 | 10.54 | 5.30 | 8.08 | 9.39 | 10.65 | 14.76 | 3.05 |
| | Ice2 | 78.90 | 49.05 | 19.17 | 14.77 | 18.02 | 10.28 | 38.01 | 8.93 | 13.55 | 9.88 | 9.63 | 9.71 | 23.33 | 9.12 |
| | Sea-Ice | 73.47 | 52.14 | 35.42 | 31.75 | 33.87 | 22.95 | 37.75 | 24.76 | 31.32 | 26.80 | 26.65 | 25.20 | 35.17 | 5.02 |
| | Ocean | 95.90 | 21.78 | 94.89 | 9.97 | 42.36 | 11.09 | 89.19 | 6.76 | 11.10 | 8.02 | 7.57 | 7.89 | 33.88 | 26.42 |
| T/P | Ocean | — | — | 66.33 | 38.78 | 11.44 | 12.49 | 17.41 | 4.53 | 6.35 | 5.48 | 5.61 | 7.08 | 17.55 | 10.37 |
| ERS-2 | Ice1 | 24.58 | 30.84 | 28.21 | 14.09 | 9.72 | 8.70 | 13.86 | 14.55 | 14.29 | 12.79 | 11.90 | 13.51 | 16.42 | 2.32 |
| | Ice2 | 50.67 | 59.77 | 46.69 | 15.08 | 12.32 | 9.04 | 23.67 | 15.25 | 14.23 | 15.53 | 13.62 | 15.50 | 24.28 | 4.71 |
| GFO | Ocean | 51.78 | 101.20 | 132.81 | 8.64 | 7.17 | 10.73 | 33.65 | 6.03 | 6.21 | 5.09 | 5.54 | 6.61 | 31.29 | 10.88 |
| Jason-1 | Ice | — | — | 17.42 | 8.53 | 5.38 | 6.48 | 47.91 | 4.29 | 6.00 | 4.41 | 5.72 | 6.68 | 11.28 | 13.25 |
| | MLE4 | — | — | 124.98 | 8.67 | 5.55 | 4.33 | 17.57 | 4.65 | 5.37 | 3.56 | 5.26 | 6.88 | 18.68 | 5.50 |
| ~~ENVISatE~~ NVISAT | Ice1 | 16.26 | 14.69 | 12.66 | 3.16 | 4.41 | 5.15 | 7.55 | 3.95 | 6.08 | 5.92 | 5.09 | 8.01 | 7.74 | 1.67 |
| | Ice2 | 20.22 | 16.30 | 27.01 | 3.32 | 4.97 | 4.90 | 9.60 | 4.40 | 4.55 | 4.33 | 3.87 | 6.00 | 9.12 | 2.15 |
| | Sea-Ice | 32.45 | 24.77 | 30.35 | 4.15 | 6.83 | 6.36 | 11.64 | 5.25 | 5.11 | 5.81 | 4.33 | 6.52 | 11.96 | 2.78 |
| | Ocean | 35.25 | 40.17 | 29.14 | 4.83 | 9.48 | 7.73 | 21.25 | 4.06 | 7.51 | 5.85 | 4.16 | 6.49 | 14.66 | 5.44 |
| Jason-2 | Ice | — | — | 17.61 | 11.97 | 7.06 | 6.41 | 7.05 | 4.37 | 7.31 | 5.28 | 6.79 | 7.92 | 8.18 | 2.02 |
| | MLE4 | — | — | 99.91 | 44.94 | 5.14 | 6.88 | 10.87 | 5.17 | 5.28 | 3.59 | 4.64 | 5.81 | 19.22 | 12.74 |
| SARAL | Ice1 | 15.41 | 23.69 | 6.77 | 3.28 | 4.91 | 4.09 | 6.00 | 4.25 | 10.23 | 3.44 | 7.62 | 4.96 | 7.89 | 2.26 |
| | Ice2 | 13.69 | 26.13 | 10.05 | 2.05 | 3.26 | 2.91 | 9.93 | 3.60 | 6.78 | 1.92 | 3.23 | 4.02 | 7.30 | 2.62 |
| | Sea-Ice | 12.56 | 35.21 | 23.96 | 2.50 | 2.76 | 2.98 | 7.94 | 3.02 | 5.39 | 2.30 | 3.48 | 4.14 | 8.85 | 2.33 |
| | Ocean | 26.11 | 29.31 | 28.23 | 2.80 | 3.39 | 4.00 | 9.39 | 3.28 | 7.88 | 2.63 | 4.02 | 4.47 | 10.46 | 2.89 |
| Jason-3 | Ice | — | — | 24.65 | 17.20 | 5.65 | 4.44 | 6.05 | 3.19 | 4.76 | 4.15 | 4.89 | 5.36 | 8.03 | 4.02 |
| | MLE4 | — | — | 110.32 | 24.02 | 3.78 | 4.51 | 4.00 | 4.83 | 5.00 | 3.24 | 5.02 | 6.82 | 17.15 | 6.98 |
| Sentinel-3 | Ice-Sheet | 11.24 | 28.38 | 12.04 | 2.58 | 3.43 | 3.04 | 9.11 | 4.81 | 4.26 | 2.69 | 2.26 | 3.89 | 7.31 | 2.23 |
| | Ice1 | 9.35 | 21.46 | 5.17 | 2.12 | 3.25 | 2.56 | 11.13 | 3.61 | 4.51 | 1.45 | 3.77 | 4.60 | 6.08 | 2.74 |
| | SAMOSA2~~3~~ | 8.25 | 23.68 | 5.14 | 2.85 | 3.79 | 3.75 | 11.07 | 6.22 | 4.48 | 3.06 | 2.56 | 4.01 | 6.57 | 2.56 |
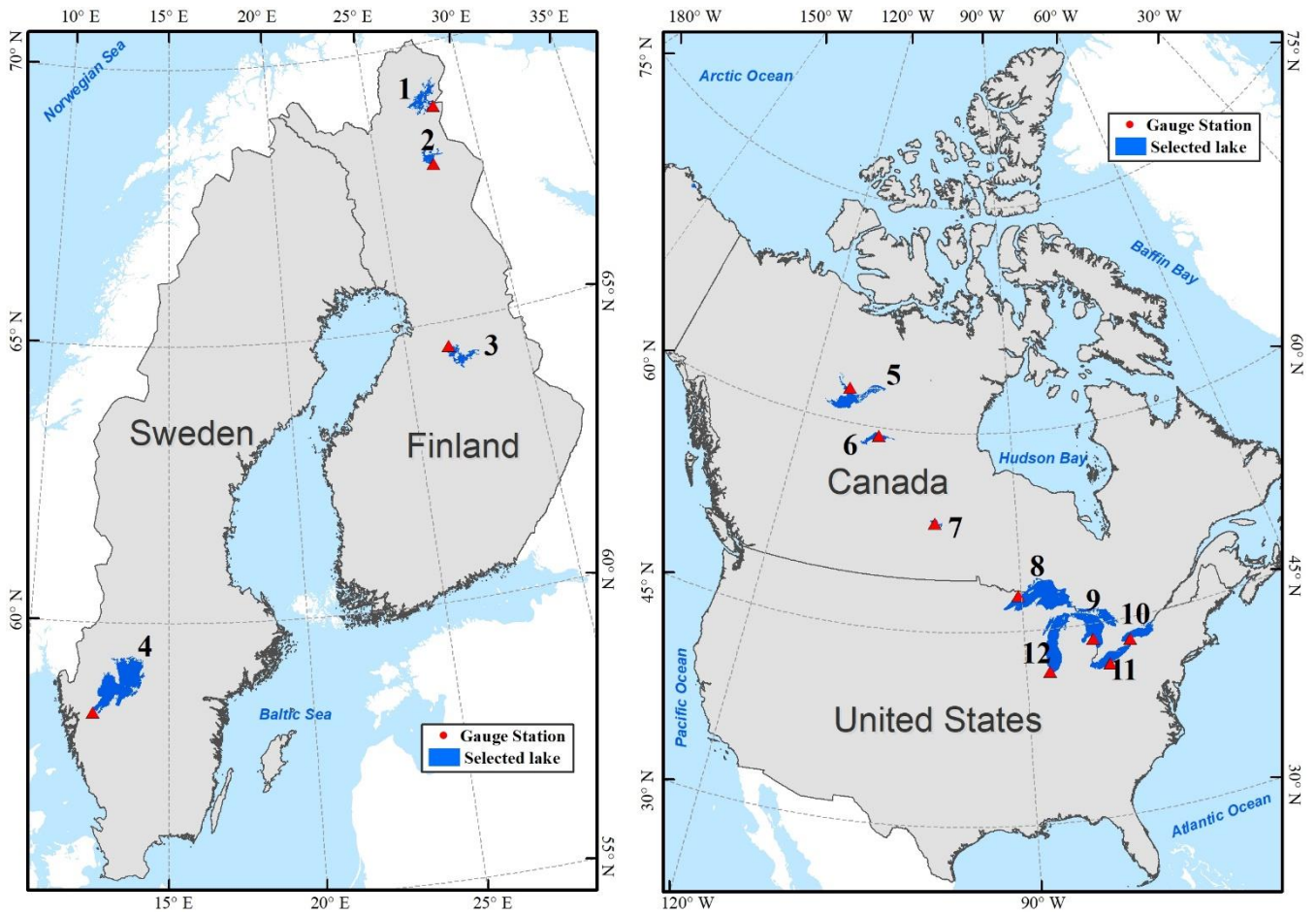
930    **Figure 1**. Geographic distribution of the case study lakes. Lakes are labelled with an identification number listed in Table 1. This figure is adapted from Fig 1 in (Shu et al., 2020).
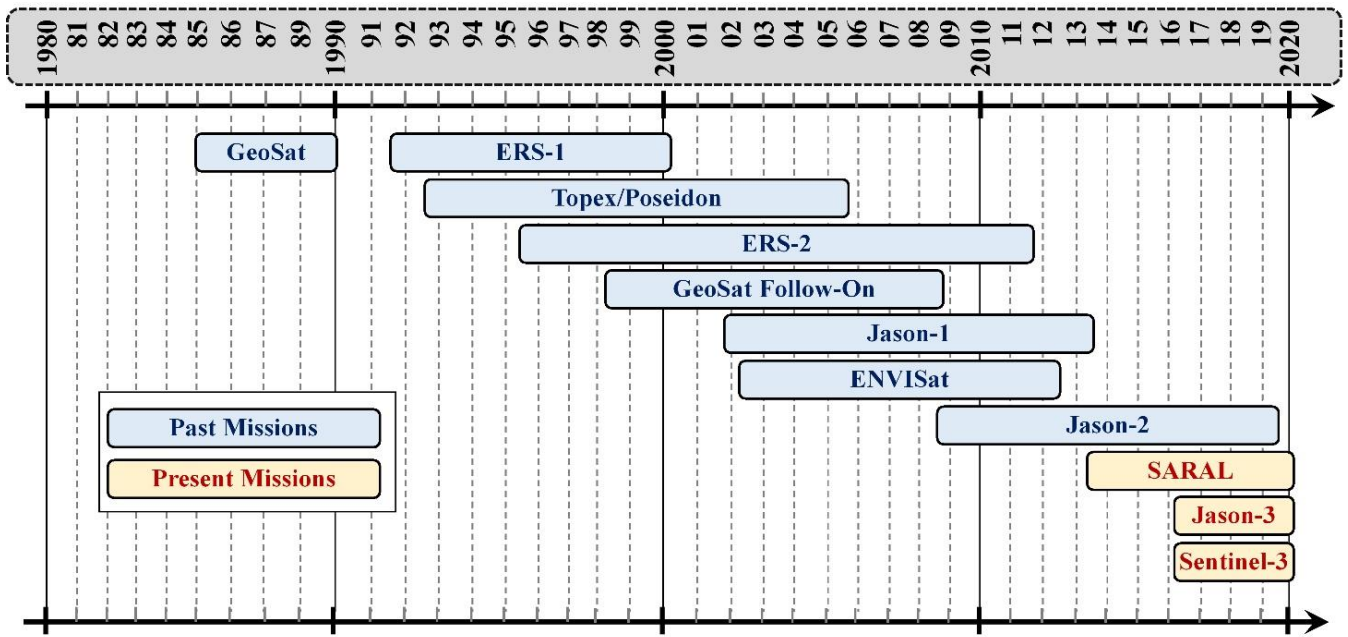
**Figure 2.** Timeline of the eleven satellite radar altimetry missions

935
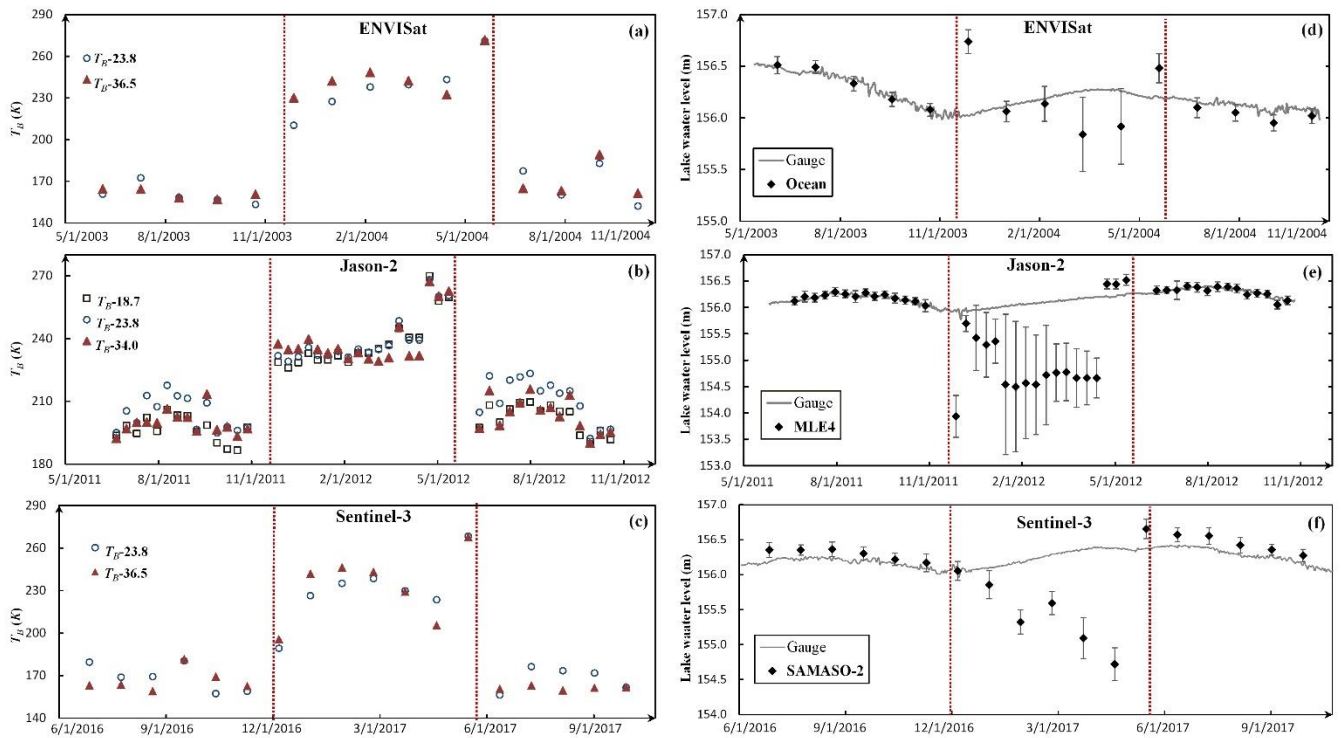
**Figure 3**. Time series of mean brightness temperature ($T_B$) and lake level estimates produced by ~~ENVISat~~ENVISAT, Jason-2 and Sentinel-3 over Great Slave Lake in the winters. (a) $T_B$ in 2003/2004 winter, (b) $T_B$ in 2011/2012 winter, (c)$T_B$ in 2016/2017 winter, (d) lake level estimate in 2003/2004 winter, (e) lake level estimates in 2011/2012 winter; and (f) lake level estimates in 2016/2017 winter.
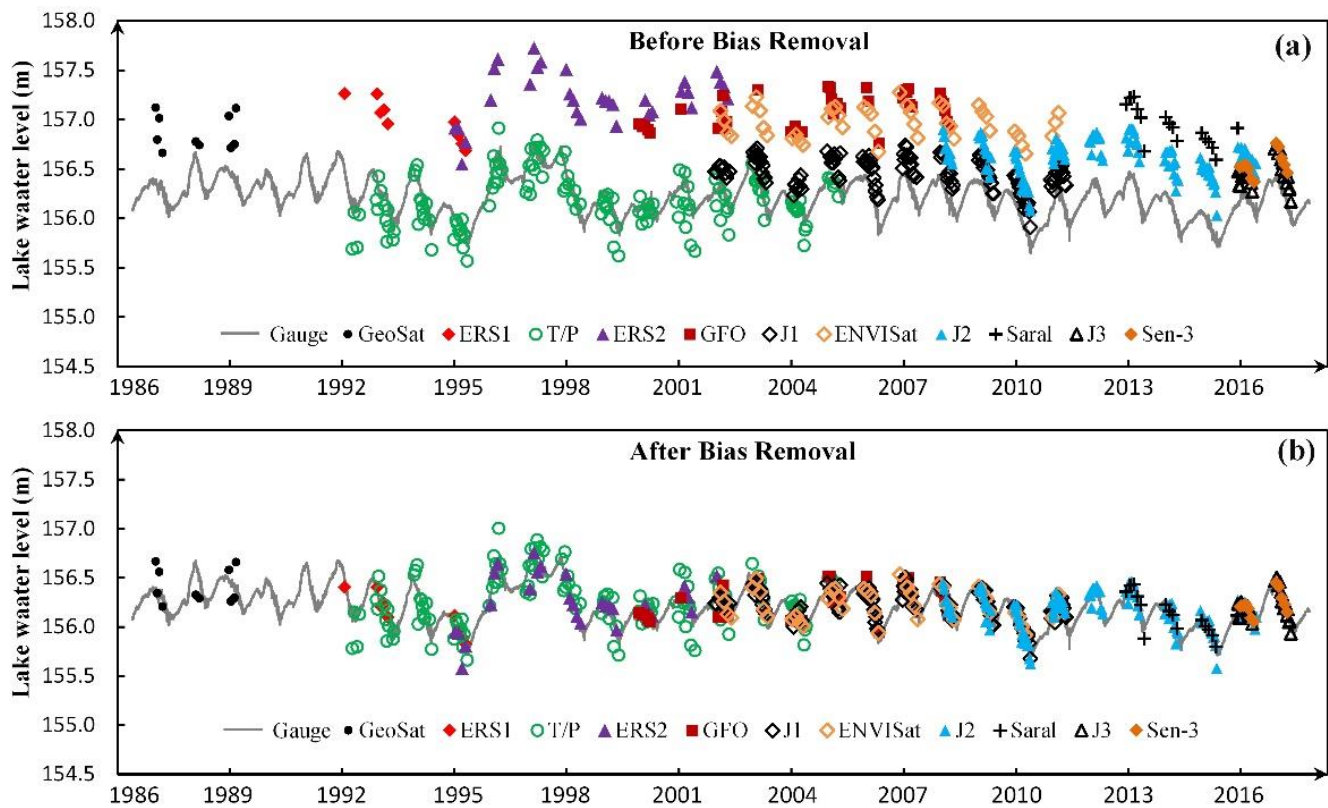
**Figure 4**. The long-term time series of lake water level derived from the eleven satellite radar altimetry missions for Great
Slave Lake in Canada; (a) the *Biases* between altimetry-derived estimates and *gauge* measurements were not removed; (b) the *Biases* were removed.
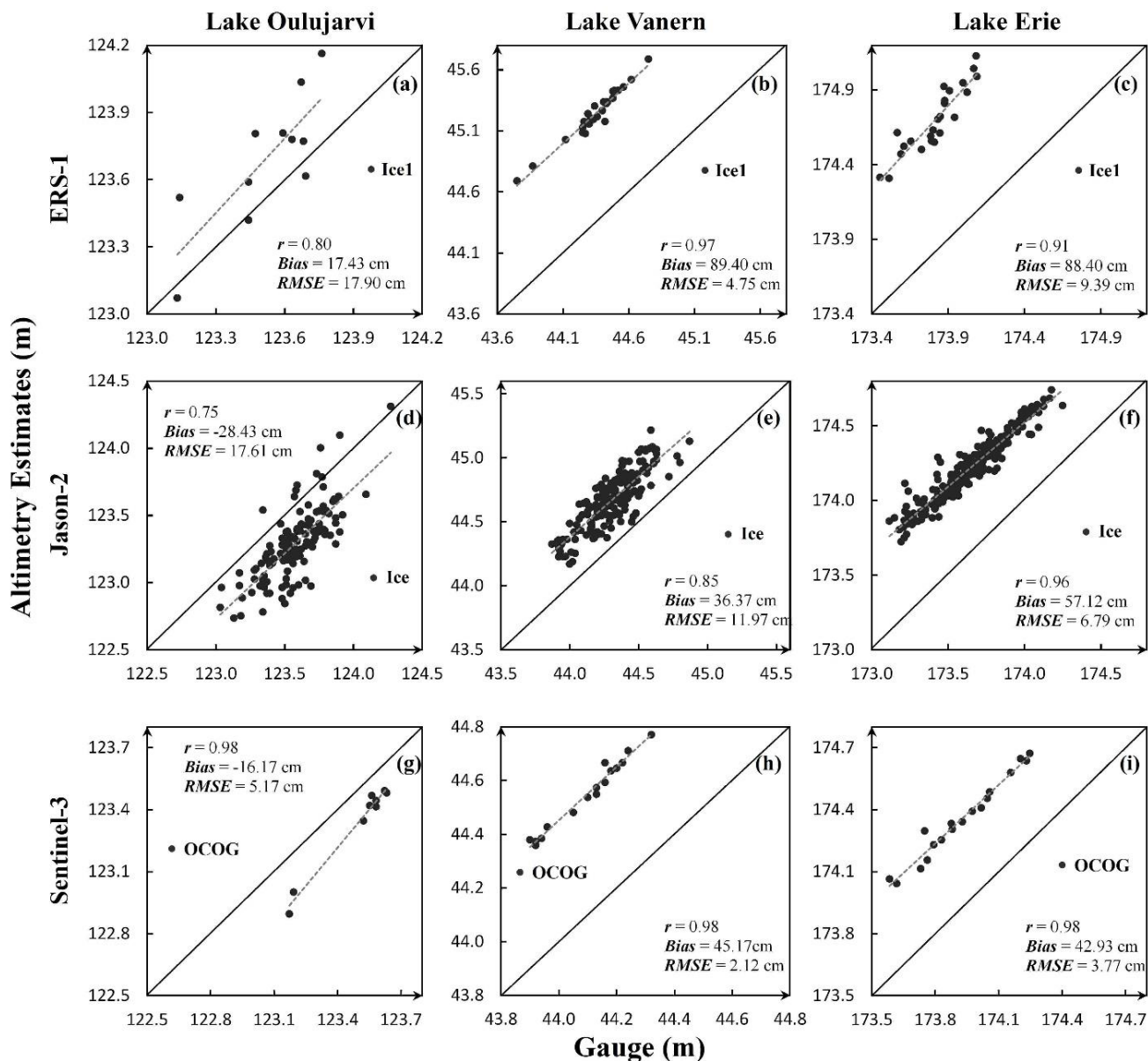
**Figure 5**. Scatterplots of lake water level estimates given by model-free retrackers against *gauge* measurements. The scatterplots of the same mission are arranged in the same row and the scatterplots of the same lake are arranged in the same column.
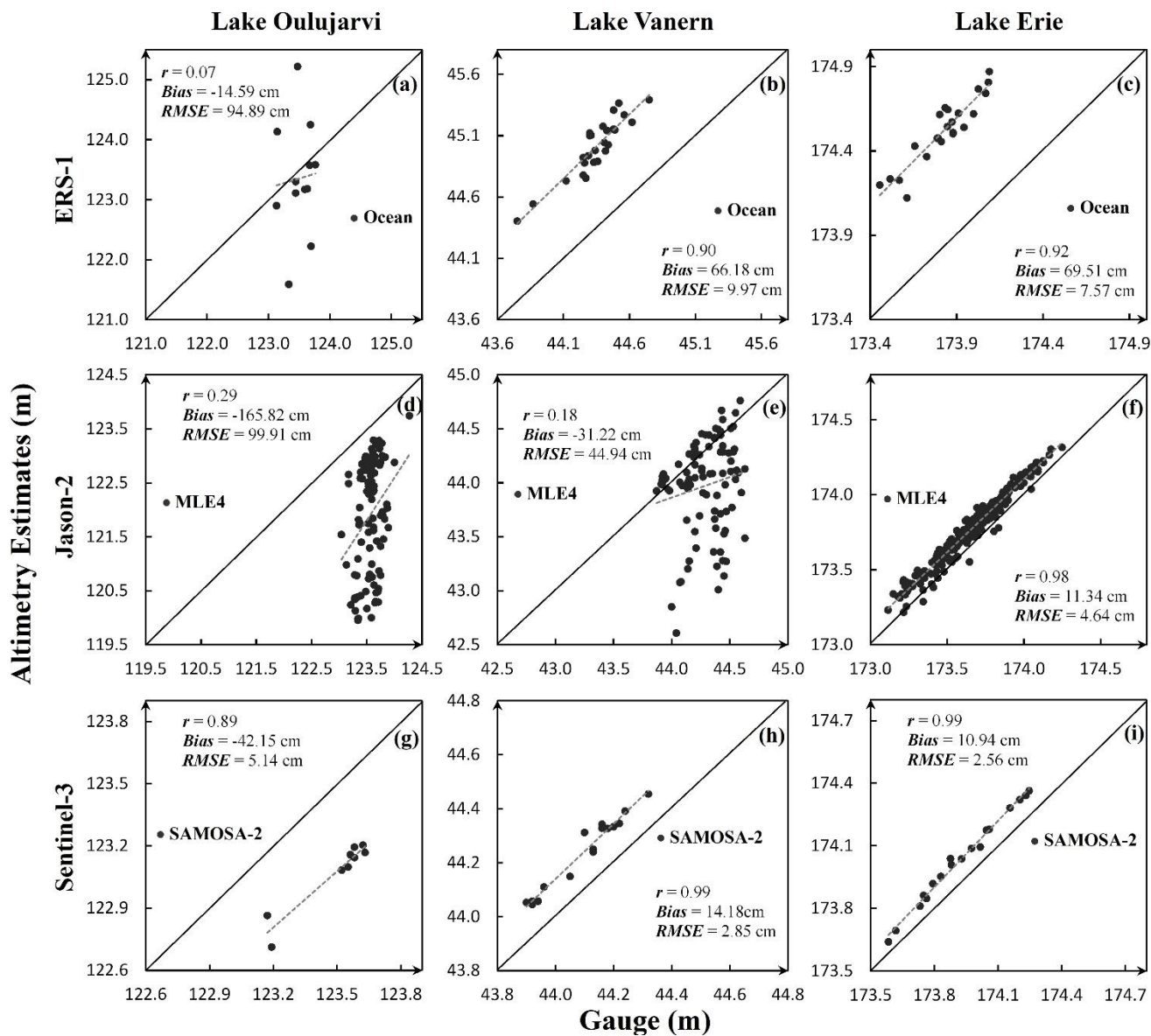
**Figure 6**. Scatterplots of lake water level estimates given by model-based retrackers against *gauge* measurements. The scatterplots of the same mission are arranged in the row and the scatterplots of the same lake are arrange in the column.

955